

Lead Isotopic Study of Young Volcanic Rocks from Mid-Ocean Ridges, Ocean Islands and Island Arcs

S.-S. Sun

Phil. Trans. R. Soc. Lond. A 1980 **297**, 409-445
doi: 10.1098/rsta.1980.0224

Email alerting service

Receive free email alerts when new articles cite this article - sign up in the box at the top right-hand corner of the article or click [here](#)

To subscribe to *Phil. Trans. R. Soc. Lond. A* go to: <http://rsta.royalsocietypublishing.org/subscriptions>

Lead isotopic study of young volcanic rocks from mid-ocean ridges, ocean islands and island arcs

By S.-S. SUN

C.S.I.R.O., Division of Mineralogy, Delhi Road, North Ryde, New South Wales, Australia 2113

Lead isotopic compositions of young volcanic rocks from different tectonic environments have distinctive characteristics. Their differences are evaluated within the framework of global tectonics and mantle differentiation. Ocean island leads are in general more radiogenic than mid-ocean ridge basalt (m.o.r.b.) leads. They form linear trends on lead isotopic ratio plots. Many of the trends extend toward the field of m.o.r.b. On plots of $^{207}\text{Pb}/^{204}\text{Pb}$ against $^{206}\text{Pb}/^{204}\text{Pb}$, their slopes are generally close to 0.1. Island arc leads in general are confined between sediment and m.o.r.b. type leads with slopes of *ca.* 0.30 on a plot of $^{207}\text{Pb}/^{204}\text{Pb}$ against $^{206}\text{Pb}/^{204}\text{Pb}$.

Pb, Sr and Nd isotopic data of Hawaiian volcanics are closely examined. Data from each island support a two-component mixing model. However, there is a lack of full range correlation between islands, indicating heterogeneity in the end members. This mixing model could also be extended to explain data from the Iceland–Reykjanes ridge, and from 45° N on the Atlantic Ridge.

The observed chemical and isotopic heterogeneity in young volcanic rocks is considered to be a result of long-term as well as short-term mantle differentiation and mixing. Lead isotopic data from ocean islands are interpreted in terms of mantle evolution models that involve long-term (more than 2 Ga) mantle chemical and isotopic heterogeneity. Incompatible element enriched ‘plume’-type m.o.r.b. have Th/U ratios *ca.* 3.0 too low and Rb/Sr ratios *ca.* 0.04 too high to generate the observed ^{208}Pb and ^{87}Sr respectively for long periods of time. Elemental fractionation in the mantle must have occurred very recently. This conclusion also applies to mantle sources for ocean island alkali basalts and nephelinites. Depletion of incompatible elements in m.o.r.b. sources is most probably due to continuous extraction of silicate melt and/or fluid phase from the low-velocity zone throughout geological time.

Data on Pb isotopes, Sr isotopes and trace elements on volcanic rocks from island arcs are evaluated in terms of mixing models involving three components derived from (1) sub-arc mantle wedge, (2) dehydration or partial melting of subducted ocean crust, and (3) continental crust contamination.

In contrast to the relation between $^{87}\text{Sr}/^{86}\text{Sr}$ and $^{143}\text{Nd}/^{144}\text{Nd}$ ratios of ocean volcanics, there is a general lack of correlation between Pb and Sr isotopic ratios except that samples with very radiogenic Pb ($^{206}\text{Pb}/^{204}\text{Pb} \geq 19.5$) have low $^{87}\text{Sr}/^{86}\text{Sr}$ ratios (0.7028–0.7035). These samples also have inferred source Th/U ratios (3.0–3.5) not high enough to support long-term growth of ^{208}Pb . Data suggest that their mantle sources have long-term integrated depletion in Rb, Th, U and light r.e.e. High $^{238}\text{U}/^{204}\text{Pb}$ (μ) values required by the Pb isotopic data are most probably due to depletion of Pb by separation of a sulphide phase. Relations between Pb, Sr and Nd isotopic ratios of young volcanic rocks could be explained by simultaneous upward migration of silicate and/or fluid phase and downward migration of a sulphide phase in a differentiating mantle.

1. INTRODUCTION

The existence of geochemical and isotopic heterogeneities in the Earth’s mantle is now well established. Variation exists among mantle derived volcanic rocks from the same tectonic settings, such as mid-ocean ridges at the spreading centres, ocean islands in the intra-plate

environments and island arcs at the consuming plate margins. In addition, samples from each different tectonic setting as a group also have their own distinctive characteristics (see, for example, Gast, 1968; Tatsumoto 1966*a*, 1978; Kay *et al.* 1970, 1978; Kay & Gast 1973; Sun & Hanson 1975*a*, 1976; De Paolo & Wasserburg 1976; O'Nions *et al.* 1977).

At present, major issues and aims in the study of mantle heterogeneity using methods of radiogenic isotopes such as Pb, Sr and Nd include:

- (1) mapping the regional distribution of such heterogeneity among volcanic products of deep-seated origin, and defining its magnitude;
- (2) defining the nature of heterogeneity in time and space throughout the Earth's history;
- (3) a better understanding of the causes of the heterogeneity in terms of processes such as melt or fluid phase migration in the mantle, magma extraction and mantle–continental crust interaction;
- (4) relating differences observed in different tectonic environments to mantle dynamics (e.g. convection, diapirism, mixing and lithosphere subduction), thermal history, mantle structure and mantle differentiation under different pressure, temperature and fluid phase conditions;
- (5) deciphering the timing and processes involved in the major evolution events of the Earth, such as core formation and mantle differentiation;
- (6) developing a unified model for the evolution of the Earth.

In this paper, new data on Pb isotopic compositions and U, Th and Pb abundances are presented for young volcanic rocks from three mid-ocean ridges, three island arcs and twelve ocean islands. Data for ocean sediments from the Atlantic Ocean, the north Philippine Sea and the north coast of California and Aleutian and Ryukyu trenches are also reported. These data are then used, along with other geochemical and isotopic data (Sr and Nd) on young volcanic rocks, to discuss various issues concerning mantle heterogeneity. Additional constraints in developing models also come from studies of older volcanic rocks and cosmochemical arguments on the composition of the bulk Earth and mantle.

2. ANALYTICAL METHODS

Powdered samples were prepared by standard methods for Pb isotopic analysis. Chemical separation of U, Th and Pb was carried out by hydroxide coprecipitation and anion exchange techniques (Tatsumoto 1966*b*; Oversby 1969). Further purification was done on small 'clean up' columns. A detailed description of the method used is available on request. Most samples were prepared in a clean laboratory in Johnson Space Center, N.A.S.A., Houston, during 1971–3. All chemicals used were prepared by using the sub-boiling method (Mattinson 1972). Total Pb blank per analysis was in the range of 5–10 ng while the Pb sample analysed was never less than 2 µg. Samples from Tristan da Cunha, Easter, Fernando de Noronha and Cape Verde Islands were prepared at the State University of New York, Stony Brook, during 1974–5 under similar conditions (Sun & Hanson 1975*b*).

Fully automated 12 inch (*ca.* 30 cm) radius, 90° sector N.B.S. design mass spectrometers were used for the isotopic measurements. Pb samples were analysed with the single filament, silica gel method (see, for example, Tatsumoto 1978) with a run temperature between 1200 and 1300 °C. Standard deviation within one set of seven ratios is generally close to 0.01%. Isotopic fractionation was carefully monitored by repeated analyses of N.B.S. standard reference sample SRM 982 and each batch of silica gel was independently calibrated. Based on replicate

analyses of SRM 982 (38), C.I.T. standard Pb (5), BCR-1 (3) and duplicate analyses of most samples used in this study (Sun 1973), the absolute uncertainty of any determination is believed to be better than $\pm 0.05\%$ per atomic mass unit. An average of five measurements on C.I.T. Pb standard gave:

$$^{206}\text{Pb}/^{204}\text{Pb} = 16.637 \pm 0.010, \quad ^{207}\text{Pb}/^{204}\text{Pb} = 15.482 \pm 0.010 \text{ and}$$

$$^{208}\text{Pb}/^{204}\text{Pb} = 36.300 \pm 0.030 (2\sigma).$$

These values agree well with those reported by Catanzaro (1967). In this paper, only average values for each sample are reported.

In the early stages of this study, the double spike method described by Compston & Oversby (1969) was used for C.I.T. standard Pb and Canary Island samples. Perfect agreement between results derived from this method and the method with SRM 982 as a mass fractionation monitor indicates that the more delicate double spike method is not a necessity for accurate determinations.

Many rock samples used by Oversby & Gast (1970) and Oversby *et al.* (1971) were reanalysed in this study. Four samples were further checked at the Isotope Geology Branch, U.S.G.S. Denver (see tables 2 and 5). Considerable disagreement exists between Oversby's data and mine (Sun 1973). Oversby (1973, personal communication) suggests that samples that she analysed might have been contaminated during sample preparation and agrees that data of the present study are more likely to be correct. A further support to this conclusion comes from the original sulphide lead data on samples from Gough and St Helena Islands analysed by Gast *et al.* (1964) and Gast (1969). Their data agree better with my data after correction for mass fractionation effect which is about -0.3% per atomic mass unit difference for the PbS method.

3. BRIEF SAMPLE DESCRIPTION

(a) *Mid-ocean ridges*

Petrological descriptions and major element geochemistry of samples from Pacific and Atlantic Oceans used in this study have been given in Kay *et al.* (1970), Miyashiro *et al.* (1969) and Engel & Engel (1964). Sample NMNH 112373 comes from the Smithsonian collection. Samples from the Indian Ocean were described by Vinogradov *et al.* (1969).

(b) *Ocean islands*

A location map of the Atlantic islands is given in figure 1.

(i) *Canary Islands*. The geology of this island group has been recently reviewed by Schmincke (1975). The total volume of volcanics in these islands is the second largest in the Atlantic next to Iceland. The eastern islands (Lanzarote and Fuerteventura) are built on the continental rise of NW Africa, while a normal oceanic crust lies beneath the western Canary Islands, i.e. La Palma, La Gomera, Hierro and Tenerife. Gran Canaria lies at the centre of this island group. Volcanism on the Canary Archipelago has been complex, as reflected in the diversity of rock types and types of volcanism. The volcanics themselves are principally alkaline and under-saturated and belong to the basanite-trachyte-phonolite assemblage. K-Ar dating (Abdel-Monem *et al.* 1971, 1972) indicates that volcanism has occurred for at least 35 Ma.

Thirty-six samples from the Canary Islands were selected for Pb isotope analysis. Ages of these samples range from 20 Ma to Recent. Petrological descriptions for most of these samples can be found in Abdel-Monem *et al.* (1971, 1972) and Oversby *et al.* (1971).

(ii) *St. Helena*. Its geology has been studied in some detail by Baker (1969). The exposed rocks belong to the alkali basalt–trachyte–phonolite assemblage. Samples used in this study come from a collection of Daly (1927) and Baker (1969). They have previously been analysed by Gast (1969) and Oversby (1969).

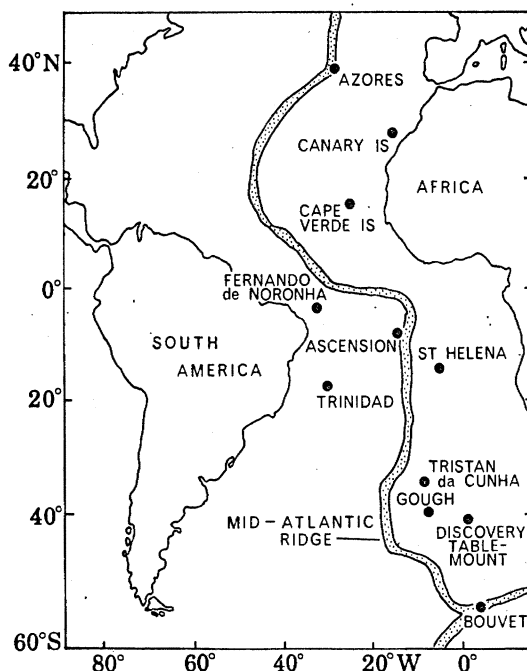


FIGURE 1. Location map of Atlantic Ocean islands.

(iii) *Azores*. The geology and geochemistry of volcanic rocks from this island group have been recently studied in detail by White (1977) and Flower *et al.* (1976). Five samples used in this study were collected by J. F. Walker.

(iv) *Ascension Island*. Its geology has been described by Daly (1925). The ages of exposed rocks are younger than 1.5 Ma (Bell *et al.* 1967). Volcanic rocks on this island belong to a basalt–trachyte–andesite–rhyolite assemblage. Four samples originally studied by Gast *et al.* (1964) are reanalysed.

(v) *Tristan da Cunha, Gough and Discovery Tablemount*. Tristan da Cunha island group (figure 1) is located about 500 km east of the Mid-Atlantic Ridge and about 370 km NNW of Gough Island. Discovery Tablemount is some 850 km east of Gough Island. The geology of Tristan da Cunha and Gough Island have been described by Baker *et al.* (1964) and Le Maitre (1962). Their volcanic rocks belong to an alkali basalt–trachybasalt–trachyte–phonolite assemblage. Tristan da Cunha samples used in this study were collected by the Royal Society Expedition 1962 (Baker *et al.* 1964). Sample TR230 is from the Stony Hill eruption (*ca.* 500 years old) and has previously been analysed by Oversby (1969). Samples TR1, 3, 4 and 6 were made available from the Smithsonian collection with original numbers 110014, 110016, 110017 and 110019. TR1 and TR3 are trachyandesite from the 1961 eruption and the latest flow beneath it. Gough

Island samples used in this study have previously been analysed by Gast *et al.* (1964) and Oversby (1969). The 25 Ma old alkali basalt sample from Discovery Tablemount used in this study has been described by Kempe & Schilling (1974).

(vi) *Bouvet Island*. It is located at a triple junction of the mid-ocean ridge system connecting the Atlantic and Indian Oceans. Three alkali basalts used in this study are from the British Museum *Discovery II* collection and they have been described by Kempe (1973).

(vii) *Cape Verde Islands*. The geological setting of these islands is similar to that of the Canary Islands (Schmincke 1975; Klerkx *et al.* 1974). Two samples used here come from British Museum Collection 1915, 130 series. The basalt sample is from the active volcano Fogo and the phonolite sample is from Praia, San Thiago.

(vii) *Fernando de Noronha*. Its geology has been described by Almeida (1958). Two samples used here are from the Rat Island. They belong to Challenger specimens of the British Museum Collection.

Three Pacific suites:

(ix) *Oahu and Kauai of Hawaiian islands*. Alkali basalts and nephelinites from the post-erosional Honolulu series of Oahu island are younger than 1 Ma and from the Koloa series of Kauai island are younger than 1.5 Ma (see, for example, McDougall 1964). Samples used in this study have been described by Kay & Gast (1973).

(x) *Guadalupe*. It is located at 29° N near the Pacific coast of Mexico. The geology and geochemistry of the volcanic rocks from this island have recently been described by Batiza (1977). Four alkali basalts used here were previously analysed by Tatsumoto (1966a).

(xi) *Easter Island*. The geology and geochemistry of Easter Island volcanics have been recently described by Baker & Buckley (1974). Bonatti *et al.* (1977) presented additional geochemical data. Two samples used in this study come from Cerro Tautapu and Rano Roraka. They are from the Smithsonian collection.

(c) *Island arcs*

(i) *Taiwan*. Taiwan (figure 2) is located between the Ryukyu arc and the Philippine arc and bounded on the east by a left-lateral strike-slip fault zone (Eastern Taiwan Longitudinal Valley, E.T.L.V.). On the eastern side of the E.T.L.V., in the Shiukuan River area, there are calc-alkaline volcanics (mainly andesites and diorites) of Miocene and probably to Pliocene age. Two small islets, Liutao and Lanhsu, off the eastern coast, also have andesites of Miocene age (Yen 1958). An ophiolite complex consisting of basaltic pillow lavas, gabbros, and serpentinites occur in the Taitung area (Shih *et al.* 1972; Liou 1974). The age of these rocks is unknown. Late Pliocene to Pleistocene volcanics on the northern part of Taiwan (Tatun and Keelung Volcano Groups and Tsaoingshan area) are related to the subduction of the Philippine Sea Plate along the Ryukyu Trench (Yen 1970). Miocene basalts in Chiaopanshan area and Pleistocene plateau basalts (tholeiite and alkali basalts) on the Penghu Islands, between Taiwan and Mainland China, are apparently not related to the island arc volcanism. These rocks are similar to Ocean Island basalts (Chen 1973; Lo & Goles 1976). Twenty-nine samples from Taiwan have been analysed in this study. They were collected by T.-P. Yen, C.-N. Yang, C.-H. Chen and L.-P. Tan.

(ii) *The Aleutian Islands*. This island arc is an arcuate chain of islands built on the Aleutian Ridge extending more than 3000 km from the Alaska peninsula on the east to the Kamchatka peninsula on the west. It is bounded by the Bering Sea to the north and the Aleutian Trench to the south. To the west of the Bering Shelf intersection, the arc is entirely within an oceanic

region. The oldest rock reported is of Eocene age (Scholl *et al.* 1970). To the east of the Bering Shelf intersection, the crust is thicker and basement rocks are as old as Mesozoic (Reed & Lanphere 1973). Kay (1977, 1978) and Kay *et al.* (1978) have made a detailed geochemical and isotopic (Pb and Sr) study of volcanic rocks from the Aleutian islands and Alaska peninsula. The same specimens were used in this study for U, Th and Pb concentration determinations.

(iii) *Tonga Islands*. The geology and geochemistry of this oceanic island arc have been recently reviewed by Ewart *et al.* (1977). Four samples used in this study are from Kao and Late. They were collected by W. Metranovas in 1966.

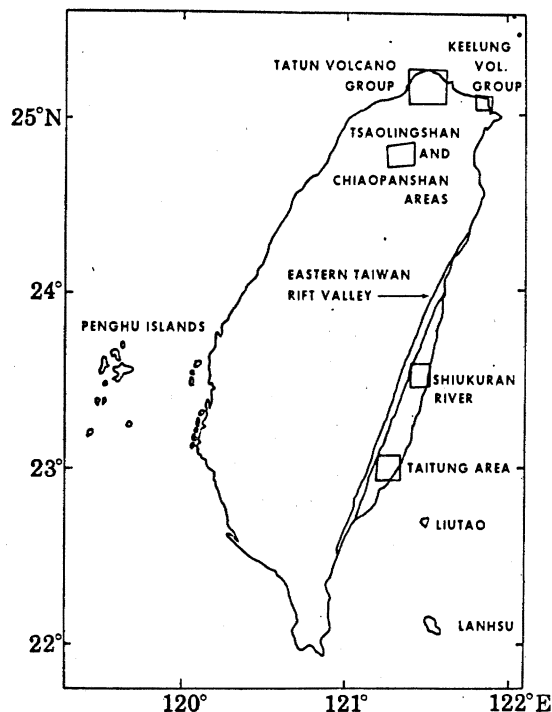


FIGURE 2. Sample location map of Taiwan.

(d) *Sediments*

Samples used in this study are from the collection of Lamont-Doherty Geological Observatory, Columbia University. They are all from triggerweight gravity cores. The location and depth of each sample are given in tables 4 and 8.

4. RESULTS

(a) *Mid-ocean ridges*

Lead isotope results are presented in table 1 and illustrated in figure 3. Fields for mid-ocean ridge basalts (m.o.r.b.) from normal ridge segments and the trends for m.o.r.b. from the Juan de Fuca ridge are also shown. The m.o.r.b. field covers a range of 17.70–18.70 for $^{206}\text{Pb}/^{204}\text{Pb}$, 15.43–15.53 for $^{207}\text{Pb}/^{204}\text{Pb}$ and 37.15–38.20 for $^{208}\text{Pb}/^{204}\text{Pb}$. Data for samples KD11 (= KD9) and 1154 from the Gorda ridge have also been reported by Church & Tatsumoto (1975). Their values agree with the present data within stated error limits. Six samples from the Vema 25

dredge haul analysed in this study have very similar Pb isotopic compositions and lie on linear trends (figure 3). Duplicate analyses of each sample show agreement better than 0.07% for $^{207}\text{Pb}/^{204}\text{Pb}$ ratios except for sample V25-1-3. The linear trends in figure 3 are likely to be real rather than a result of mass fractionation during analysis.

TABLE 1. LEAD ISOTOPE COMPOSITIONS OF VOLCANIC ROCKS FROM MID-OCEAN RIDGES

sample	$^{206}\text{Pb}/^{204}\text{Pb}$	$^{207}\text{Pb}/^{204}\text{Pb}$	$^{208}\text{Pb}/^{204}\text{Pb}$	location
East Pacific Rise				
Amph D-1	18.193	15.478	37.755	7° 50' S, 108° 08' W
Amph D-3	18.160	15.459	37.664	12° 52' S, 110° 57' W
Amph D-4	18.588	15.534	38.174	18° 25' S, 113° 19' W
V21-40	18.348	15.500	37.914	5° 31' S, 106° 46' W
KD-11	18.404	15.505	37.879	42° 50' N, 126° 55' W
1154	18.333	15.464	37.716	42° 50' N, 126° 55' W
112373	18.395	15.465	37.805	Blanco Trough (ca 43° N, 126° W)
Mid-Atlantic Ridge				
V25-1-103	18.311	15.466	37.694	25° 24' N, 45° 18' W
V25-1-97	18.323	15.482	37.733	25° 24' N, 45° 18' W
V25-1-3	18.315	15.471	37.718	25° 24' N, 45° 18' W
V25-1-9	18.318	15.485	37.748	25° 24' N, 45° 18' W
V25-1-6	18.362	15.507	37.850	25° 24' N, 45° 18' W
V25-1-10	18.342	15.493	37.796	25° 24' N, 45° 18' W
A150-7-1	18.173	15.461	37.639	30° 01' N, 42° 04' W
Indian Ocean Ridge				
DP 2/1	18.122	15.500	37.988	5° 2' N, 62° 7' E
TP13/29	18.179	15.530	38.141	5° 32' S, 68° 25' E
DP 4/1	18.243	15.500	37.986	5° 2' N, 62° 1' E
DP 22/4	18.100	15.492	37.973	5° 21' S, 68° 42' E

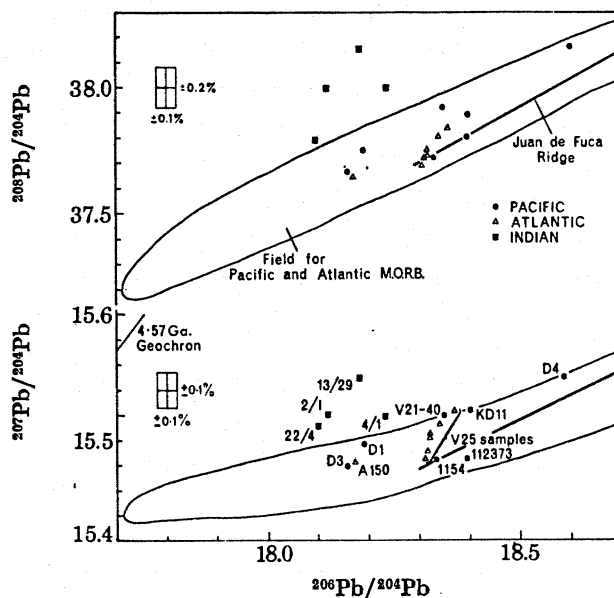


FIGURE 3. Pb isotopic composition of m.o.r.b. Fields for Pacific and Atlantic samples are based on data of Sun *et al.* (1975), Church & Tatsumoto (1975), Tatsumoto (1978), and this study. Regression lines for Juan de Fuca ridge are from Church & Tatsumoto (1975).

From figure 3 and data in the literature some observations can be made for m.o.r.b.:

1. Their total range of variation in Pb isotopic ratios is much smaller than ocean island lead (figure 9).

2. They are less radiogenic than most ocean island leads and are closer to the 4.57 Ga Geochron (Tatsumoto *et al.* 1973), with future ages (i.e. they plot to the right of the Geochron).

3. 'Normal' m.o.r.b. from the Pacific and Atlantic oceans cover similar ranges in Pb isotopic compositions. This is consistent with Sr isotope data from both oceans with $^{87}\text{Sr}/^{86}\text{Sr}$ ratios ranging from 0.7023 to 0.7028 (Hart 1976; Sun *et al.* 1979). In contrast, four Indian Ocean m.o.r.b. analysed in this study appear to have higher $^{207}\text{Pb}/^{204}\text{Pb}$ and $^{208}\text{Pb}/^{204}\text{Pb}$ ratios (figure 3). More accurate data on Indian Ocean samples are required to confirm this observation.

4. M.o.r.b. from a restricted area, such as Juan de Fuca and Gorda ridges (Church & Tatsumoto 1975), Reykjanes ridge (Sun *et al.* 1975, and figure 17), and 45° N Mid-Atlantic Ridge (Sun *et al.* 1980), tend to show linear trends on Pb isotopic ratio plots. Their slopes on a plot of $^{207}\text{Pb}/^{204}\text{Pb}$ against $^{206}\text{Pb}/^{204}\text{Pb}$ are generally close to 0.10, which is also the trend for most ocean islands.

(b) Ocean islands

Experimental results are presented in tables 2, 3 and 5 and are further illustrated in figures 4–10. Although only average values are reported for each sample in the tables, replicate analyses are plotted in the figures.

Data from Canary Island samples are shown in figures 4 and 5. The total range of variation for $^{206}\text{Pb}/^{204}\text{Pb}$ is 5%, for $^{207}\text{Pb}/^{204}\text{Pb}$ it is 0.6%, and for $^{208}\text{Pb}/^{204}\text{Pb}$ it is 2.5%. These variations are greater than observed in other islands or island groups. The linear regression for a plot of $^{207}\text{Pb}/^{204}\text{Pb}$ against $^{206}\text{Pb}/^{204}\text{Pb}$ has a slope of 0.104 ± 0.007 (1σ). The slope for a plot of $^{208}\text{Pb}/^{204}\text{Pb}$ against $^{206}\text{Pb}/^{204}\text{Pb}$ is 0.945 ± 0.090 (1σ). Data from all seven islands fit on a single regression line. There is no clear correlation of Pb isotopic composition with geographic position, age of the samples, or rock types. When each island is considered, it occupies part of the regression line and overlaps with other islands. This could be either due to real differences in the source regions as in the Hawaiian islands (§5c), or a sampling problem. Gran Canaria, having many samples analysed, occupies almost the whole range. There is no indication that different crustal types underlying the east (continental) and west (oceanic) Canary Islands have any effect on the Pb isotopic composition of the volcanic rocks. Results of several oceanic sediments from areas surrounding the Canary Islands are also shown in figures 4 and 5 to test the possibility of sediment contamination. Pb isotopic compositions of these sediments have characteristics of ocean sediments from the Atlantic Ocean (Chow & Patterson 1962, and table 4), i.e. they have higher $^{207}\text{Pb}/^{204}\text{Pb}$ but lower $^{206}\text{Pb}/^{204}\text{Pb}$ ratios than the Canary samples. Therefore the linear trends on Pb isotopic plots for Canary samples are caused neither by contamination from the continental crust nor by the ocean sediments. It is more likely that these variation trends reflect characteristics and/or fundamental processes of the magma sources in the mantle.

Results of two samples from Cape Verde Islands (figure 6) fall on the Canary Islands trends in both plots (figures 9 and 10). Samples from these two island groups also have similar Sr isotope ratios (figure 19).

Good linear trends in Pb isotope ratio plots have also been found in basalts from the Iceland–Reykjanes ridge (Sun & Jahn 1975; Sun *et al.* 1975), the Hawaiian Islands (Tatsumoto 1978),

OCEANIC LEADS

417

TABLE 2. LEAD ISOTOPE COMPOSITIONS OF SAMPLES FROM THE CANARY ISLANDS

sample	$^{206}\text{Pb}/^{204}\text{Pb}$	$^{207}\text{Pb}/^{204}\text{Pb}$	$^{208}\text{Pb}/^{204}\text{Pb}$	rock type	age
Gran Canaria					
GCU1	19.590	15.619	39.509	basalt	
GCU21	19.540	15.591	39.486	olivine basalt	2.80 Ma
GCU23A	19.429	15.599	39.268	olivine basalt	1.96 Ma
GCU29A	19.225	15.556	39.298	tephrite	3.50 Ma
GCU64	19.746	15.635	39.592	phonolite	9.60 Ma
GC53	20.045	15.663	39.893	phonolite	10.30 Ma
GCU32	19.735	15.620	39.513	separated feldspar	13.30 Ma
CL13	19.498	15.616	39.290	—	
GCU14	19.500	15.610	39.244	plagioclase basalt	15.70 Ma
GCU15	19.548	15.632	39.370	trachyrhyolite	15.00 Ma
GCU6	19.594	15.630	39.375	separated feldspar	13.10 Ma
Lanzarote					
LZ137	19.230	15.576	39.058	basalt	1730–1736 A.D.
LZ139	19.254	15.570	39.034	basalt	1730–1736 A.D.
LZ17260 (a)†	19.109	15.559	38.922	alkali basalt	—
LZ17260 (b)	19.115	15.573	38.921	—	—
LZ110	19.243	15.577	39.066	olivine basalt	0.96 Ma
LZU8	19.199	15.565	39.017	tholeiitic basalt	1730–1736 A.D.
LZ105	19.573	15.601	39.380	basanite	7.68 Ma
LZ3	19.447	15.610	39.369	picritic basalt	10.60 Ma
LZ106	19.204	15.565	39.018	trachybasalt	19.00 Ma
Fuerteventura					
FV18	19.339	15.597	39.141	olivine basalt	4.25 Ma
FV4	19.761	15.620	39.588	augite basalt	15.88 Ma
FV23	19.607	15.616	39.436	plagioclase basalt	20.00 Ma
Tenerife					
TF67	19.810	15.632	39.669	alkali trachyte	0.53 Ma
TF104	19.752	15.641	39.663	pholoite	0.24 Ma
TFAR	19.673	15.620	39.472	olivine basalt	1705 A.D.
TF86	20.022	15.661	39.918	trachyte	5.35 Ma
TF96	19.684	15.605	39.495	phonolite	< 1 Ma
TF85	19.860	15.641	39.578		
Hierro					
H7	19.460	15.603	39.141	olivine basalt	0.19 Ma
H16	19.602	15.604	39.270	plagioclase basalt	0.74 Ma
La Palma					
LP26	19.874	15.644	39.644	olivine basalt	0.81 Ma
LP19A	19.616	15.588	39.366	augite basalt	1808 A.D.
LP9A	19.616	15.598	39.396	augite basalt	1808 A.D.
LP15	19.583	15.620	39.463	phonolite	0.60 Ma
La Gomera					
LG150	19.987	15.641	39.626		
LG58	19.766	15.612	39.357	olivine basalt	4.69 Ma
LZ137‡	19.203	15.556	39.030		
TFAR‡	19.645	15.590	39.407		
FV23‡	19.585	15.597	39.379		

† This is the same sample used by Zartman & Tera (1973). Zartman (1975, oral communication) agrees that the data of this study are more likely to be correct.

‡ Samples analysed in Denver by U.S.G.S.

TABLE 3. ABUNDANCES OF Pb, U AND $^{238}\text{Pb}/^{204}\text{Pb}$, $^{232}\text{Th}/^{238}\text{U}$ RATIOS OF SOME CANARY ISLAND SAMPLES

sample	[Pb]/($\mu\text{g/g}$)	[U]/($\mu\text{g/g}$)	[Th]/($\mu\text{g/g}$)	$^{238}\text{U}/^{204}\text{Pb}$	$^{232}\text{Th}/^{238}\text{U}$
GCU21	4.98	1.95	8.70	26	4.6
GCU29A	7.47	3.38	13.6	29	4.2
GCU53	28.5	10.9	44.5	25	4.2
GCU15	6.16	1.54	5.63	16	3.8
LG150	3.00	1.33	5.09	29	4.0
LZ137	1.37	0.524	2.04	25	4.0
TFAR	n.d.	1.01	4.11	n.d.	4.2
LZ17260†	3.1	1.55	5.88	32	3.9

† Data from Zartman & Tera (1973).

TABLE 4. LEAD ISOTOPE COMPOSITIONS OF SOME ATLANTIC OCEAN SEDIMENTS

sample no.	latitude	longitude	$^{206}\text{Pb}/^{204}\text{Pb}$	$^{207}\text{Pb}/^{204}\text{Pb}$	$^{208}\text{Pb}/^{204}\text{Pb}$	depth cm
V22-170	14° 38' S	07° 34' W	19.011	15.716	39.075	10-13
V22-171	13° 06' S	09° 20' W	18.995	15.705	39.076	23-25
V23-96	29° 48' N	15° 06' W	18.837	15.670	38.938	6-10
V23-97	24° 07' N	17° 26' W	18.879	15.700	39.058	7-10
V23-95	30° 24' N	18° 23' W	18.989	15.708	39.132	19-23
V27-143	39° 43' N	20° 09' W	19.072	15.707	39.150	47-50
V27-159	33° 59' N	13° 20' W	18.865	15.681	38.949	33-35
V27-142	30° 60' N	22° 54' W	19.112	15.689	39.202	15-17
V27-166	25° 51' N	22° 43' W	18.934	15.691	39.080	43-47
V27-176	07° 11' N	25° 22' W	18.890	15.712	39.130	36-40
V22-93	09° 55' N	20° 58' W	18.872	15.723	39.214	46
V25-72	09° 31' N	51° 58' W	19.020	15.704	39.096	42-71
V24-258	02° 21' N	43° 18' W	18.966	15.730	39.114	50
V25-58	00° 04' N	32° 48' W	18.884	15.691	38.969	71

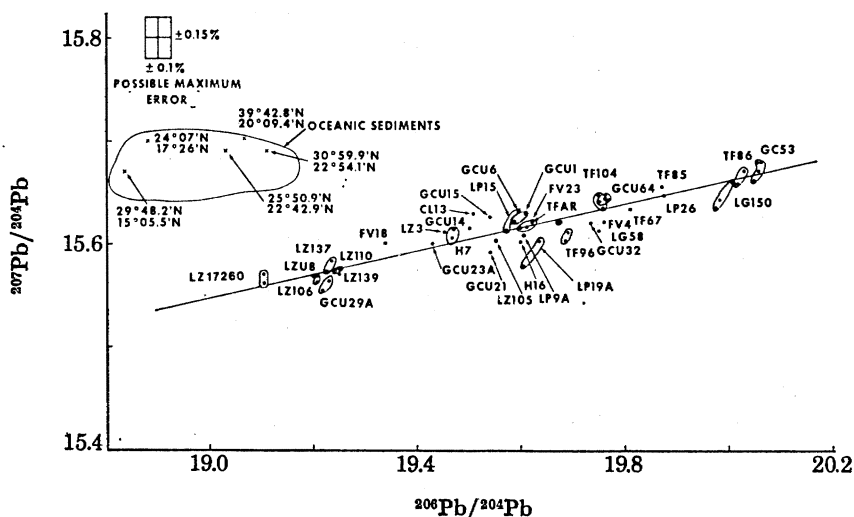


FIGURE 4. Results for samples from Canary Islands on a plot of $^{207}\text{Pb}/^{204}\text{Pb}$ against $^{206}\text{Pb}/^{204}\text{Pb}$. The regression line has a slope of 0.104 ± 0.007 (1σ) which corresponds to a two stage model age of 1.70 ± 0.12 Ga.

Juan de Fuca–Gorda ridges and nearby seamounts (Church & Tatsumoto 1975) and Ross Island, Antarctica (Sun & Hanson 1975*b*). They have very similar slopes on Pb isotope ratio plots (figures 9 and 10). Their regression trends also point towards the general field of m.o.r.b.

Samples from the Azores (except Faial 373) and Ascension islands have Pb isotopic compositions and variation trends similar to samples from the Canary Islands and Ross Island (figures 9 and 10). Four samples from Faial (Oversby 1971, and Faial 373 of this study) have considerably (0.3–0.7%) higher $^{207}\text{Pb}/^{204}\text{Pb}$ ratios than expected from the Canary Islands trend. In

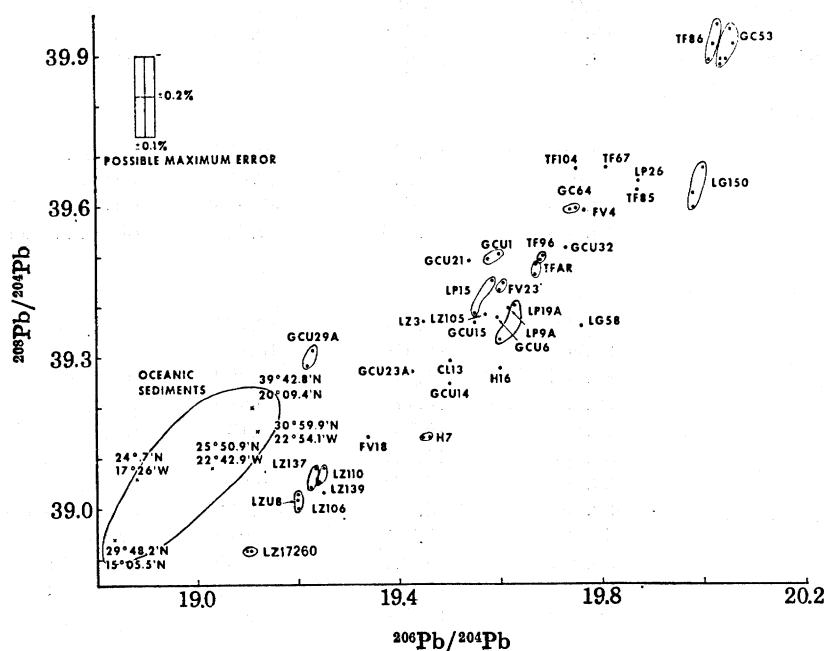


FIGURE 5. Results for samples from Canary Islands on a plot of $^{208}\text{Pb}/^{204}\text{Pb}$ against $^{206}\text{Pb}/^{204}\text{Pb}$.

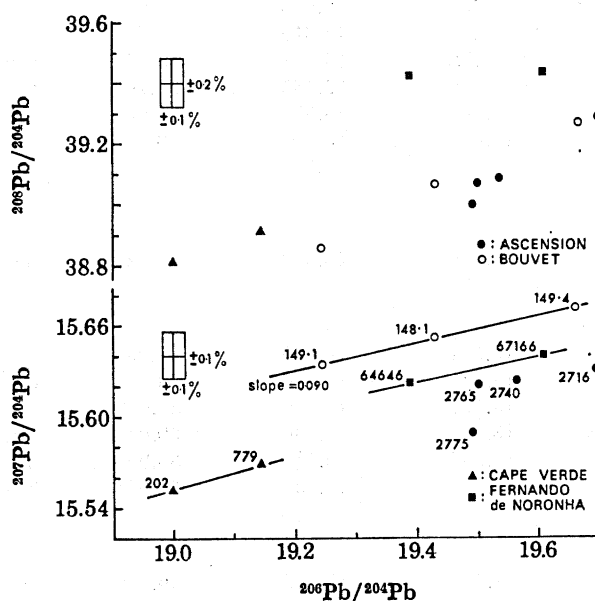


FIGURE 6. Lead isotope data for samples from Bouvet, Cape Verde, Fernando de Noronha and Ascension Islands.

TABLE 5. LEAD ISOTOPE COMPOSITIONS OF SAMPLES FROM AZORES, ASCENSION, ST HELENA, GOUGH, DISCOVERY TABLEMOUNT, TRISTAN DA CUNHA, BOUVET, CAPE VERDE, FERNANDO DE NORONHA, OAHU, KAUAI, EASTER AND GUADALUPE ISLANDS

sample	$^{206}\text{Pb}/^{204}\text{Pb}$	$^{207}\text{Pb}/^{204}\text{Pb}$	$^{208}\text{Pb}/^{204}\text{Pb}$	rock type
Azores				
Faial 373	19.561	15.641	39.225	trachy basalt
Flores 3F/196	19.954	15.638	39.545	trachyte
San Jorge 332	19.964	15.637	39.405	basalt
Terceira 200	19.617	15.606	39.153	basalt
Santa Maria 6	19.561	15.606	39.375	basalt
Ascension Island				
2716	19.716	15.630	39.278	trachyte
2740	19.566	15.626	39.092	basalt
2765	19.503	15.625	39.069	olivine basalt
2775	19.486	15.590	39.010	obsidian bomb
St Helena				
2882	20.896	15.791	40.131	olivine basalt
2928	20.908	15.810	40.161	basalt
2935	20.822	15.790	40.092	phonolite
2933	20.827	15.778	40.089	phonolite
2894	20.830	15.797	40.131	trachy basalt
2878	20.739	15.782	40.077	plagioclase basalt
237/5†	20.709	15.786	40.005	basalt
167	20.797	15.806	40.133	phonolitic trachyte
662	20.701	15.786	40.015	phonolitic trachyte
11	20.814	15.787	40.085	phonolite
145	20.801	15.783	40.085	olivine basalt
2894§	20.800	15.776	40.089	
Gough				
G95	18.323	15.598	38.793	trachy basalt
G111	18.552	15.606	39.045	olivine basalt
G8	18.295	15.610	38.739	basalt
G18	18.622	15.602	39.143	trachyte
G15	18.280	15.585	38.766	andesite
G132‡	18.30	15.59	38.69	basalt
G19D‡	18.47	15.60	39.02	trachyte
G3‡	18.64	15.60	39.14	trachyte
Discovery Tablemount				
BM1954, 152	18.246	15.609	38.723	basalt
Tristan da Cunha				
TR230	18.547	15.529	39.035	trachy-andesite
TR2.2	18.587	15.546	39.065	trachy-andesite
TR1	18.537	15.519	38.940	trachy-andesite
TR3	18.567	15.530	39.044	trachy-andesite
TR4	18.504	15.515	38.965	basalt
TR6	18.566	15.523	39.031	basalt
Bouvet				
148(1)	19.428	15.652	39.066	basalt
149(1)	19.245	15.633	38.855	basalt
149(4)	19.661	15.672	39.273	basalt†

OCEANIC LEADS

421

TABLE 5 (cont.)

sample	$^{206}\text{Pb}/^{204}\text{Pb}$	$^{207}\text{Pb}/^{204}\text{Pb}$	$^{208}\text{Pb}/^{204}\text{Pb}$	rock type
Cape Verde				
202	18.996	15.552	39.807	phonolite
779	19.144	15.570	38.913	basalt
Fernando de Noronha				
64646	19.393	15.622	39.427	nephelinite
67166	19.609	15.641	39.431	nephelinite
Oahu				
023	18.160	15.466	37.800	nephelinite
035	18.166	15.465	37.811	nephelinite
021	18.158	15.469	37.831	nephelinite
043	18.143	15.464	37.778	nephelinite
024	18.164	15.465	37.811	nephelinite
04	18.166	15.466	37.816	alkali basalt
Kauai				
K22	18.114	15.460	37.754	nephelinite
K16	18.157	15.446	37.754	nephelinite
K17	18.136	15.450	37.854	nephelinite
K23	18.362	15.460	38.045	nephelinite
K24	18.247	15.450	37.970	gabbro
Easter Island				
26	18.789	15.560	38.392	felsite
13	19.290	15.573	38.839	felsite
Guadalupe				
GU22	20.038	15.619	40.019	alkali basalt
GU44	20.088	15.615	40.106	alkali basalt
GU52	20.176	15.612	40.150	alkali basalt
GU77	20.303	15.635	40.263	alkali basalt

† Analysed by S. E. Church.

‡ Data from Gast *et al.* (1964). Corrections for mass fractionation effect by PbS method (0.2–0.4 % per atomic mass unit) are made by adjusting $^{207}\text{Pb}/^{204}\text{Pb}$ values of these samples to conform with data of this study.

§ Sample analysed in Denver by U.S.G.S.

addition, detailed Sr and Pb isotopic studies by White *et al.* (1976) and Dupré *et al.* (1978) on samples from the Azores reveal a complicated picture. It is possible that four samples of this study from Flores, San Jorges, Terceira and Santa Maria falling on the Canary trends are fortuitous.

Five nephelinites and one alkali basalt from the Honolulu series of Oahu Island have identical Pb isotopic composition within analytical error limits, whereas samples from Koloa series of Kauai Island have a spread of 1 % in $^{206}\text{Pb}/^{240}\text{Pb}$ ratio. Data from these two islands reported here also conform with data from other Hawaiian islands (Tatsumoto 1978, and figures 15 and 16). Discussion on Hawaiian data will be presented in § 5c.

St Helena samples (table 5, figure 7) have the most radiogenic leads among ocean volcanics. Both basalt and phonolites cover the same limited fields of variation, i.e. less than 1 % variation in $^{206}\text{Pb}/^{204}\text{Pb}$ ratios. Pb isotopic data support the field observation (Baker 1969) that basalts and phonolites from St Helena could be related by crystal fractionation.

Data from Gough, Tristan da Cunha Islands and Discovery Tablemount are plotted on figure 8. Along with Hawaiian and Kerguelan (Dosso 1977) and Cook Island (Swainbank 1967) samples, they have the lowest $^{206}\text{Pb}/^{204}\text{Pb}$ ratios among ocean islands. In spite of their having similar $^{206}\text{Pb}/^{204}\text{Pb}$ ratios to m.o.r.b., their $^{208}\text{Pb}/^{204}\text{Pb}$ ratios are much higher than m.o.r.b., suggesting an evolution history with high Th/U ratio (*ca.* 4.0). Samples from Gough Island and Discovery Tablemount fall on the same regression lines on Pb isotope ratio plots. The slope of $\Delta^{207}\text{Pb}/\Delta^{206}\text{Pb}$ on a plot of $^{207}\text{Pb}/^{204}\text{Pb}$ against $^{206}\text{Pb}/^{204}\text{Pb}$ (figure 8) is very shallow

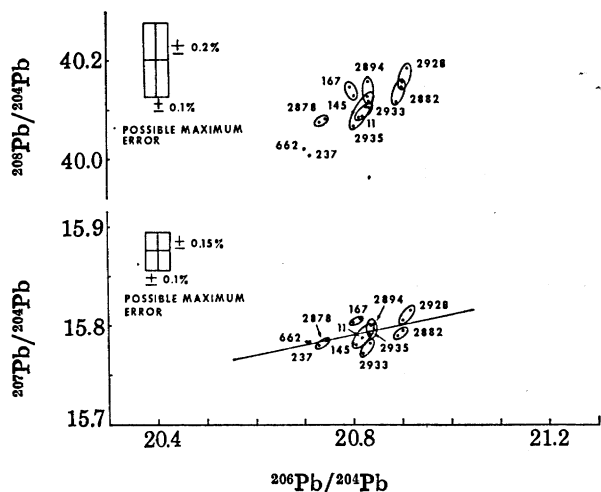


FIGURE 7. Lead isotope data for samples from St Helena.

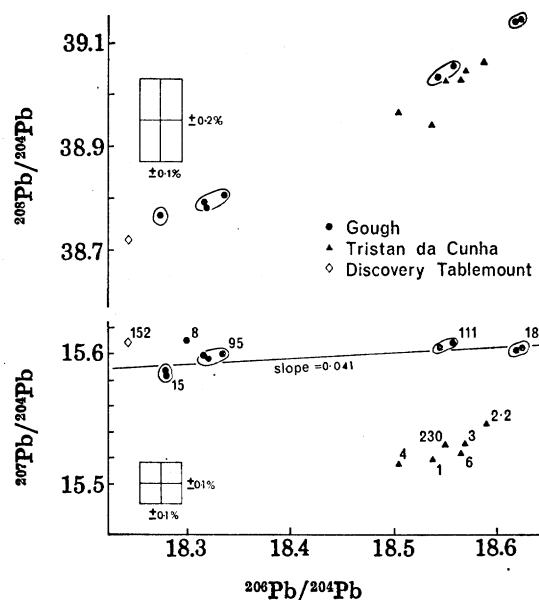


FIGURE 8. Lead isotope data for samples from Gough, Tristan da Cunha and Discovery Tablemount.

(not more than 0.04). They also have the same Sr isotope ratios of *ca.* 0.7050 (Sun, unpublished data). Available Pb and Sr isotope data seem to support the suggestion made by Kempe & Schilling (1974) that Gough Island and Discovery Tablemount have the same type of mantle source. Samples from Tristan da Cunha have limited variation in Pb isotope ratios. This is consistent with limited variation in $^{87}\text{Sr}/^{86}\text{Sr}$ ratios reported by O'Nions & Pankhurst (1974). $^{207}\text{Pb}/^{204}\text{Pb}$ ratios of samples from Tristan da Cunha are systematically *ca.* 0.5% lower than those of Gough Island and Discovery Tablemount, suggesting that Tristan samples have been developed under environment with lower $^{238}\text{U}/^{204}\text{Pb}$ (μ) ratio.

Some observation can be made on characteristics of oceanic island lead:

1. There is considerable overall variation: 17% in $^{206}\text{Pb}/^{204}\text{Pb}$ ratio, 7% in $^{208}\text{Pb}/^{204}\text{Pb}$ ratio and 2.5% in $^{207}\text{Pb}/^{204}\text{Pb}$ ratio. At a particular $^{206}\text{Pb}/^{204}\text{Pb}$ ratio of 18.2, $^{207}\text{Pb}/^{204}\text{Pb}$ ratios vary from 15.43 to 15.60 and $^{208}\text{Pb}/^{204}\text{Pb}$ ratios vary from 37.6 to 38.9. These variations must reflect different mantle evolution histories, including variation in U/Pb and Th/U ratios in different mantle domains. Observed $^{238}\text{U}/^{204}\text{Pb}$ ratios in near-primary alkali basalts in ocean islands range from 15 to 30 and there is a crude correlation with $^{206}\text{Pb}/^{204}\text{Pb}$ ratios. Observed Th/U ratios in these alkali basalts range from 3 to 5 (Tatsumoto 1966*a, b*, 1978; Oversby 1969; Swainbank 1967; this study).

2. Oceanic island lead is generally more radiogenic than m.o.r.b. lead. Exceptions include samples from Gough, Tristan da Cunha, Kerguelen Islands, Discovery Tablemount, Cook Island (Swainbank 1967) and the Hawaiian Islands. They have $^{206}\text{Pb}/^{204}\text{Pb}$ ratios similar to m.o.r.b. However, except for Hawaiian samples, they all have higher $^{207}\text{Pb}/^{204}\text{Pb}$ and especially $^{208}\text{Pb}/^{204}\text{Pb}$ ratios (2–3%) than m.o.r.b. (figures 9 and 10).

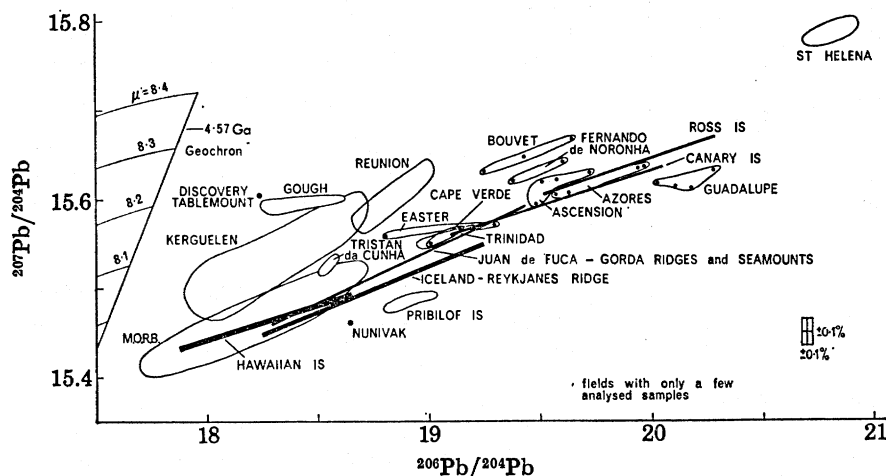


FIGURE 9. Plot of $^{207}\text{Pb}/^{204}\text{Pb}$ against $^{206}\text{Pb}/^{204}\text{Pb}$ for volcanic rocks from oceanic islands. Data sources for Reunion and Trinidad, Oversby (1971, 1972); Hawaiian Islands, Tatsumoto (1978) and this study; Pribilof Islands, Kay *et al.* (1978); Iceland and Reykjanes ridge, Sun & Jahn (1975), Sun *et al.* (1975); Ross Island, Sun & Hanson (1975*b*); Nunivak, Zartman & Tera (1975); Kerguelen, Dosso (1977). The rest are from this study.

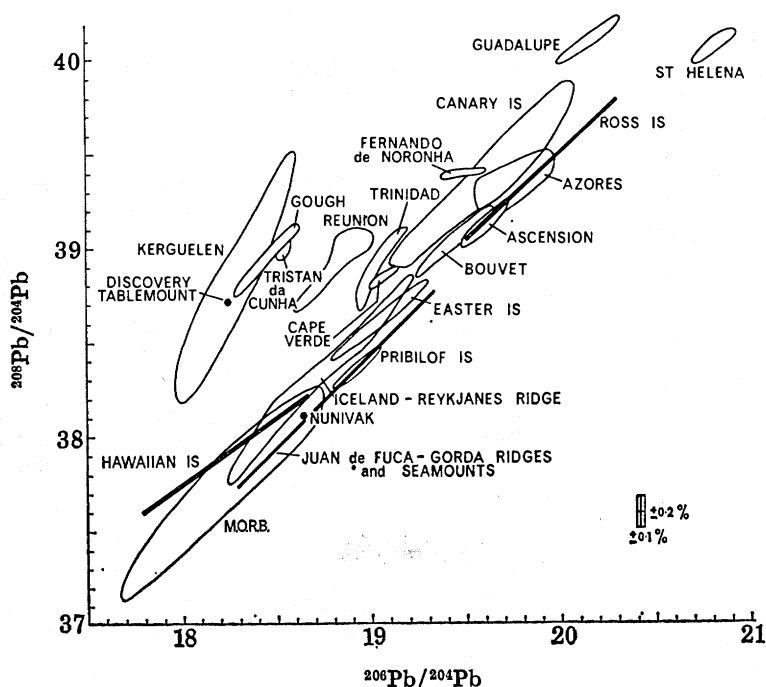


FIGURE 10. Plot of $^{208}\text{Pb}/^{204}\text{Pb}$ against $^{206}\text{Pb}/^{204}\text{Pb}$ for volcanic rocks from oceanic islands. Data sources are the same as in figure 9.

TABLE 6. LEAD ISOTOPE COMPOSITIONS OF VOLCANIC ROCKS FROM TAIWAN AND TONGA ISLANDS

sample	$^{206}\text{Pb}/^{204}\text{Pb}$	$^{207}\text{Pb}/^{204}\text{Pb}$	$^{208}\text{Pb}/^{204}\text{Pb}$	rock type
<i>Taiwan</i>				
Taitung area				
K8A1a	17.952	15.457	37.781	gabbro
K10A2b	18.060	15.461	37.698	gabbro
K11A1b	18.015	15.468	37.727	pillow basalt
TPY6458	18.005	15.450	37.788	pillow basalt
Shiukuran River area				
D-1	18.323	15.571	38.463	diorite
S16A2b	18.346	15.598	38.538	diorite
S3A2c	18.303	15.560	38.438	andesite
Lanhsu				
WLY005	18.315	15.591	38.558	andesite
WLY009	18.350	15.603	38.628	andesite
LPT2	18.398	15.620	38.750	andesite
Tatun Volcano Group				
A1	18.478	15.627	38.750	andesite
A99	18.460	15.629	38.736	andesite
A87	18.483	15.631	38.759	andesite
A17	18.483	15.633	38.759	andesite
A24	18.470	15.612	38.696	andesite
A41	18.617	18.640	38.856	andesite
B1	18.523	15.623	38.729	basalt
B5	18.450	15.607	38.700	basalt
B7	18.440	15.613	38.705	basalt
Chiaopanshan area				
TPYb71-11	18.375	15.612	38.731	basalt
TPYb71-18	18.366	15.593	38.636	basalt
Tsaolingshan				
TPYb71-15	18.465	15.640	38.791	basalt
Keelungshan Volcano Group				
G1	18.519	15.645	38.814	dacite
W1	18.504	15.622	38.758	dacite
P2	18.442	15.560	38.498	andesite
Penghu Islands				
PY234	18.745	15.557	38.828	basalt
PY60	18.684	15.589	38.821	basalt
Y123	18.686	15.588	38.869	diabase
Y122	18.710	15.610	38.875	basalt
<i>Tonga</i>				
Late				
WM1	18.564	15.540	38.137	andesite
WM2	18.555	15.556	38.155	andesite
Kao				
WM5	18.611	15.546	38.161	andesite
WM7	18.613	15.562	38.226	andesite

3. Good linear trends (figures 9 and 10) appear to be the rule instead of the exception among oceanic Pb data. Many of the linear trends point toward the m.o.r.b. field. On the plot of $^{207}\text{Pb}/^{204}\text{Pb}$ against $^{206}\text{Pb}/^{204}\text{Pb}$, the oceanic lead trends, including oceanic islands and ridges, generally have a slope of *ca.* 0.10. Exceptions include Gough and Bouvet Islands on the plot of $^{207}\text{Pb}/^{204}\text{Pb}$ against $^{206}\text{Pb}/^{204}\text{Pb}$, and Guadalupe, Reunion and Gough Islands on the plot of $^{208}\text{Pb}/^{204}\text{Pb}$ against $^{206}\text{Pb}/^{204}\text{Pb}$.

TABLE 7. ABUNDANCES OF U, Th, Pb, AND Th/U, $^{238}\text{U}/^{204}\text{Pb}$ RATIOS IN VOLCANIC ROCKS OF TAIWAN, THE ALEUTIAN ISLANDS AND NEARBY OCEANIC SEDIMENTS

	[U]/(μg/g)	[Th]/(μg/g)	[Pb]/(μg/g)	Th/U	$^{238}\text{U}/^{204}\text{Pb}$
Taiwan					
K11A1b	0.030	0.092	0.332	3.05	5.6
S3A2C	0.54	0.85	1.29	1.57	27
A1	1.60	5.10	6.93	3.18	15
A24	4.10	7.85	12.6	1.92	21
A41	2.14	6.46	8.14	3.01	16
P2	0.48	1.63	3.03	3.38	10
PY234	1.25	5.28	2.40	4.21	33
Y123	0.56	2.86	1.75	5.1	20
the Aleutians					
UM5	0.96	—	8.29	—	7.4
UM2O	1.09	2.17	7.97	1.98	8.6
UM22	0.493	0.906	5.08	1.83	6.2
B1927	1.02	2.82	3.87	2.74	16
ADK6	0.97	2.03	3.80	2.08	16
ADK53	1.30	3.02	4.16	2.31	20
ADK58	1.67	3.89	8.19	2.32	13
Ryukyu Trench floor					
V21-108	1.21	7.70	17.1	6.42	4.6
seaward of the Aleutian Trench					
RC10-199	4.21	3.27	9.31	0.77	28
RC10-208	2.54	2.52	11.0	0.99	15
off N California coast					
RC10-299	7.04	6.96	13.6	0.99	33
RC10-230	1.86	8.41	19.5	4.5	6.1

(c) *Island arcs*

Experimental results are presented in tables 6–8 and further illustrated in figures 11–14.

(i) *The Aleutian Islands.* Pb isotopic data of the Aleutian samples have been published by Kay *et al.* (1978). Figure 11 shows the relation of Pb isotopic composition among volcanic rocks and sediments from the NE Pacific region. Samples from the Juan de Fuca–Gorda ridges and associated seamounts lie between the Cascades calc-alkali volcanic belt and the Aleutian arc. Pribilof and Nunivak Islands are in the Bering Sea to the north of the Aleutian arc. On the plot of $^{207}\text{Pb}/^{204}\text{Pb}$ against $^{206}\text{Pb}/^{204}\text{Pb}$, m.o.r.b., Pribilof and Nunivak basalts define an oceanic trend with a slope of *ca.* 0.10. On the other hand, both Cascades and Aleutian samples define a much steeper trend with slope of *ca.* 0.30, which is a characteristic of arc volcanics (Tatsumoto & Knight 1969; Armstrong & Cooper 1971). In fact, the Cascades and Aleutian leads are confined between fields of the continental detritus component and m.o.r.b. Exceptions to this

relation include three magnesian andesites from Adak (ADK52, 53) and Unimak (70-B49). Their Pb isotopic compositions follow the m.o.r.b. trends. These samples also have $^{87}\text{Sr}/^{86}\text{Sr}$ ratios (0.7028–0.7029) similar to m.o.r.b. Kay (1978) suggests that they were generated by partial melting of subducted oceanic crust in eclogite facies with garnet in the residue, which also cause severe depletion of heavy r.e.e. in these samples.

TABLE 8. LEAD ISOTOPE COMPOSITION OF SEDIMENTS FROM THE RYUKYU TRENCH, THE ALEUTIAN TRENCH AND THE WEST COAST OF CALIFORNIA

sample	latitude	longitude	$^{206}\text{Pb}/^{204}\text{Pb}$	$^{207}\text{Pb}/^{204}\text{Pb}$	$^{208}\text{Pb}/^{204}\text{Pb}$	comment	depth/cm
V21-108	25° 44' N	127° 34' E	18.593	15.680	39.075	Ryukyu Trench floor	10
V21-111	24° 30' N	128° 31' E	18.615	15.647	38.869	seaward wall of Ryukyu Trench	19
V21-113	23° 40' N	128° 17' E	18.618	15.651	38.845	N Philippine Sea	15
RC10-199	51° 19' N	174° 01' W	18.944	15.623	38.631	seaward of Aleutian Trench	10
RC10-208	51° 38' N	171° 46' W	18.935	15.605	38.650	seaward of Aleutian Trench	25
RC10-229	45° 35' N	126° 09' W	19.037	15.674	39.012	off N California coast	24
RC10-230	40° 28' N	128° 25' W	19.028	15.654	38.973	off N California coast	16

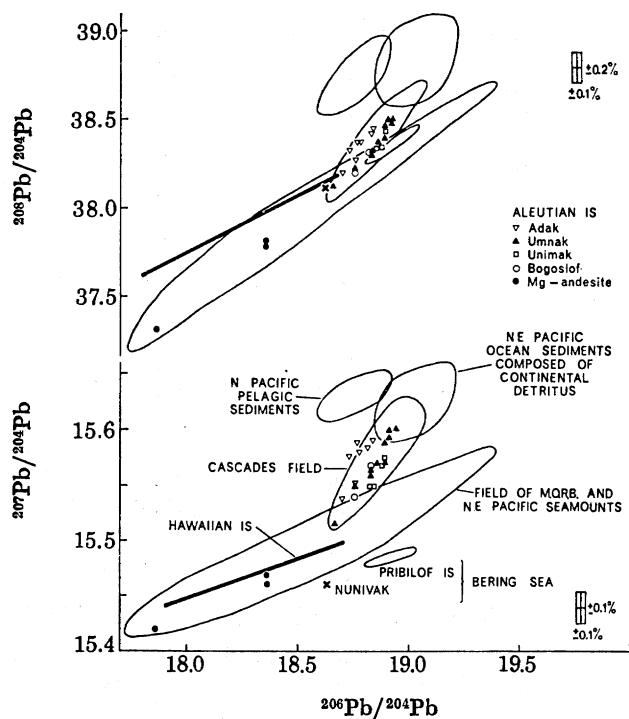


FIGURE 11. Lead isotope data for samples from the Aleutian islands and surrounding areas. Data are from Sun (1973), Kay *et al.* (1978), Kay (1978), Zartman & Tera (1973), Church (1976) and Chow & Patterson (1962).

It is significant that despite different crustal structures underneath the Cascades and the eastern and western Aleutian arcs, no systematic differences in Pb isotopic composition can be suggested except that samples from Adak Island, to the west of the Bering shelf intersection, have slightly lower $^{206}\text{Pb}/^{204}\text{Pb}$ ratios. The Adak data might suggest a changing character of sediment

involvement (such as an increasing amount of pelagic sediments) away from the North American mainland. Kay *et al.* (1978) also show that among the Aleutian samples studied, no difference has been observed in Sr isotopes across the Bering Shelf intersection. Consequently they conclude that crustal contamination is not a proper explanation for the mixing trends.

Among the Aleutian samples analysed for U, Th and Pb concentration, there is an inverse correlation between $^{238}\text{U}/^{204}\text{Pb}$ and $^{206}\text{Pb}/^{204}\text{Pb}$ ratios (figure 12). Th/U ratios of the Aleutian samples range from 1.83 to 2.74.

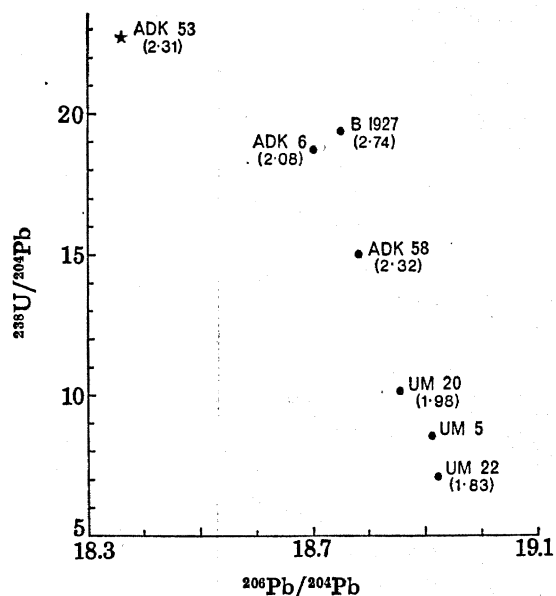


FIGURE 12. Plot of $^{238}\text{U}/^{204}\text{Pb}$ against $^{206}\text{Pb}/^{204}\text{Pb}$ for Aleutian samples. Th/U ratios are presented in parentheses. ADK53 is a basaltic andesite considered to be a melting product of the subducted oceanic crust (Kay 1978).

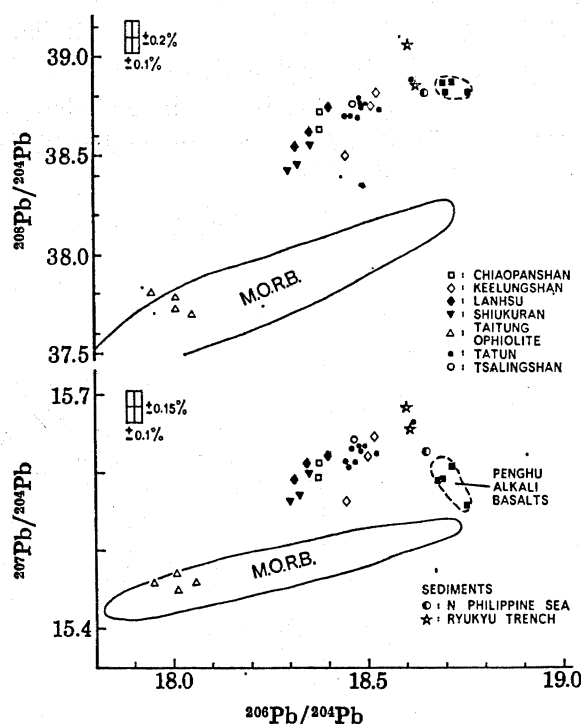


FIGURE 13. Results for samples from Taiwan on Pb isotopic ratio plots. The negative regression slope for Penghu alkali basalts is similar to Auckland alkali basalts (Armstrong & Cooper 1971).

Two andesite samples from Mexico were also analysed in this study. They are from the Museum collection of Harvard University. Their results also fall within the Cascades fields: sample 37783 from Zacatecas has $^{206}\text{Pb}/^{204}\text{Pb} = 18.658$, $^{207}\text{Pb}/^{204}\text{Pb} = 15.575$ and $^{208}\text{Pb}/^{204}\text{Pb} = 38.333$, and sample 37789 from Ixtapalapa Chalco has $^{206}\text{Pb}/^{204}\text{Pb} = 18.742$, $^{207}\text{Pb}/^{204}\text{Pb} = 15.601$ and $^{208}\text{Pb}/^{204}\text{Pb} = 38.523$.

(ii) *Taiwan*. In figure 13, ophiolitic basalts and gabbros from eastern Taiwan fall within the m.o.r.b. trend. Additional data from the same area (J. H. Chen, personal communication, 1978) also follow the m.o.r.b. trend and have $^{206}\text{Pb}/^{204}\text{Pb}$ ranging from 17.9 to 18.6. Major and trace element data of these samples (Shih *et al.* 1972; Liou 1974; Sun *et al.* 1979) further suggest that they are of m.o.r.b.-type magmas. On the same figure, Pb isotopic composition of volcanic rocks from northern Taiwan are confined between m.o.r.b. and sediments from the Ryukyu trench and North Philippine Sea. This situation is similar to other island arcs.

Pliocene–Pleistocene volcanics from the Tatunshan, Keelungshan and Tsaolingshan groups tend to be more radiogenic than Miocene volcanics from Shiukuan River area, Lanhsu and Chiaopanshan area. A progressive change of Pb isotopic composition with time has also been reported in the West Indies (Armstrong & Cooper 1971).

Plateau basalts from Penghu Islands do not fall on the trend defined by volcanic rocks on the island of Taiwan. On a plot of $^{207}\text{Pb}/^{204}\text{Pb}$ against $^{206}\text{Pb}/^{204}\text{Pb}$ they have a trend with a negative slope pointing to the ocean sediments. This situation is similar to that of Auckland alkali basalts of New Zealand studied by Armstrong & Cooper (1971). Geochemical characteristics of the Penghu basalts are also similar to ocean island basalts (Chen 1973; and this study). A reasonable explanation for the negative slope is two component mixing with crustal Pb as one end member. It is estimated that ‘uncontaminated’ Penghu basalts have $^{206}\text{Pb}/^{204}\text{Pb} \approx 18.80$, $^{207}\text{Pb}/^{204}\text{Pb} \approx 15.55$ and $^{208}\text{Pb}/^{204}\text{Pb} \approx 38.80$.

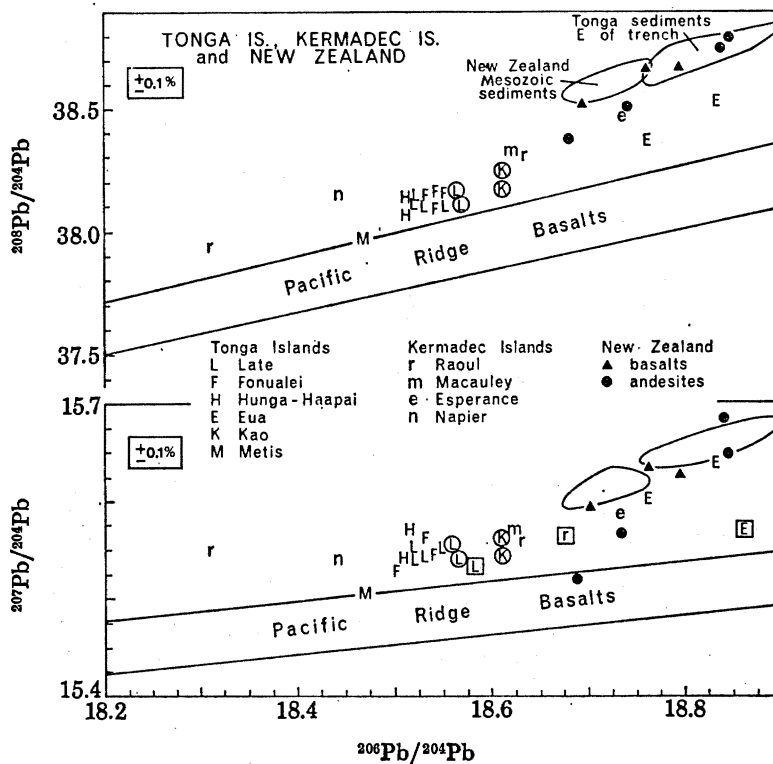


FIGURE 14. Results for samples from Tonga, Kermadec Islands and New Zealand on Pb isotopic ratio plots. ○, Analysed by Sun; □ analysed by Hart; other data are from Oversby & Ewart.

Among samples from Taiwan analysed for Th, U and Pb abundances, Th/U ratios range from 1.6 to 3.4 and $^{238}\text{U}/^{204}\text{Pb}$ from 5.6 to 27. There is no correlation between these ratios and Pb isotopic composition.

(iii) *Tonga-Kermadec and New Zealand.* Figure 14 shows that the Pb isotopic compositions of these arc volcanics are confined between the fields of m.o.r.b. and sediments from the Tonga Trench and the New Zealand mesozoic geosyncline. One possible exception is Raoul sample 7128 with $^{206}\text{Pb}/^{204}\text{Pb} = 18.31$ (Oversby & Ewart 1972). Its $^{207}\text{Pb}/^{204}\text{Pb}$ ratio is about 0.2% higher than expected from the mixing trend. Among Kermadec samples, again except for Raoul 7128, there is a tendency towards more radiogenic Pb isotopic compositions southward

towards New Zealand. In contrast there is only 0.6% variation in $^{206}\text{Pb}/^{204}\text{Pb}$ ratios among Tonga samples covering a distance of 300 km and with no consistent pattern of variation. Oversby & Ewart (1972) propose that inter-arc spreading in the Lau Basin behind the Tonga Islands has caused convective mixing and homogenization in the mantle wedge underneath the Tonga Islands.

Sinha & Hart (1972) have reported some Pb isotope and trace element data on volcanic rocks from Tonga Islands and sediments from east of the trench. Reanalyses of these samples by S. R. Hart (personal communication, 1974) indicate that considerable analytical error is involved in both isotopic and concentration measurements. For example, Pb abundances in Tonga samples are found to be 5–10 times lower than earlier reported by Sinha & Hart (1972). Consequently, their arguments against the two component mixing model will be disregarded here. New measurements of Pb isotopic composition of these samples by Hart are also plotted on figure 14. Except for the Eua sample they agree well with data reported by Oversby & Ewart (1972) and in this study.

No data are yet available on volcanic rocks within the inter-arc Lau Basin to define Pb isotopic composition of the 'uncontaminated' mantle in that region. Until samples from the Lau Basin are analysed, one could argue that Tonga–Kermadec Pb have trends parallel to the oceanic trends but with $^{207}\text{Pb}/^{204}\text{Pb}$ and $^{208}\text{Pb}/^{204}\text{Pb}$ *ca.* 0.2% higher than m.o.r.b.

Among Tonga Island samples analysed for U and Pb concentration, Oversby & Ewart (1972) show that there is a positive correlation between $^{206}\text{Pb}/^{204}\text{Pb}$ and $^{238}\text{U}/^{204}\text{Pb}$ ratios. This is in contrast to the Aleutian data presented earlier.

Modern island arc type Pb from different parts of the world share some fundamental characteristics. They all have steeper slopes in Pb isotope ratio plots than Pb from ocean island and mid-ocean ridges. They are universally confined between two components, i.e. m.o.r.b. and ocean sediment (or upper continental crust) type leads (figures 11, 12 and 14). The lead isotopic composition of each island arc also reflects the regional characteristics of oceanic sediment lead. For example, in the NE Pacific, the lead isotopic composition of volcanic rocks from the Aleutian arc, Cascades and Mexico would reach a limiting value of $^{206}\text{Pb}/^{204}\text{Pb} \approx 19.0$, which is also the average composition of continental-derived sediments in the east Pacific Ocean. In contrast, the limiting $^{206}\text{Pb}/^{204}\text{Pb}$ in the NW Pacific (Japan and Taiwan) is about 18.6, which reflects the Pb isotopic composition of sediments in that region. Island arcs within the oceanic plate far away from continental sources might be exceptions to the general observation described above. Lead isotopic compositions of samples from the Mariana and New Hebrides Islands show no indication of sediment involvement (Meijer 1976; Lancelot *et al.* 1978). A trachyandesite from Iwo Jima (Tatsumoto 1966*b*) is also an exception. It has a Pb isotopic composition $^{206}\text{Pb}/^{204}\text{Pb} = 19.44$, $^{207}\text{Pb}/^{204}\text{Pb} = 15.62$, $^{208}\text{Pb}/^{204}\text{Pb} = 39.44$ (normalized to absolute ratios) similar to oceanic island lead. The tectonic environment of Iwo Jima (see, for example, DeLong *et al.* 1975) suggests that its magma could have come from below the subducted lithosphere. Additional exceptions are two andesite samples from Dominica. Their Pb isotopic compositions are more radiogenic than average Atlantic sediments (Armstrong & Cooper 1971). Pushkar (1968) found that plagioclase separates from these andesites have $^{87}\text{Sr}/^{86}\text{Sr}$ ratios considerably lower than those of the groundmass, and he suggested that crustal contamination has changed the isotopic ratios of the magma.

5. DISCUSSION

(a) Degree of mantle heterogeneity in oceanic regions

Although it is generally accepted that the Earth's mantle is chemically heterogeneous in trace element abundances, the geometry of such heterogeneity has not yet been well defined. It could be in the form of random distribution or stratification. In contrast to the idea of mantle heterogeneity, it has been suggested that the observed isotopic heterogeneity could be mainly a result of the melting behaviour of a homogeneous source (see, for example, O'Nions & Pankhurst 1974; Church & Tatsumoto 1975). Arguments against this interpretation come from geological observations (e.g. those of Sun & Hanson 1975*a*, 1976) and trace element diffusion data (e.g. those of Hofmann & Hart 1978), which suggest that isotopic homogenization could be achieved within a short time period under partial melting conditions. A further supporting argument could be raised by considering the consequences of continuous changes in P and T conditions during mantle diapirism. Under these circumstances reorganization of mineral assemblage and/or mineral composition would enhance trace element diffusion.

There is a possibility that mantle heterogeneity is magnified by melting of 'raisin pudding' type mantle. Alkali basalts in oceanic islands generated by small degree of partial melting could have sampled only the enriched mantle domains, while m.o.r.b., generated by large degrees of partial melting, sample the bulk mantle source. Although this melting effect could be important in many cases, other geological observations suggest that regional heterogeneity on a scale of several tens to several hundred kilometres must be also important. Evidence comes from the existence of large-scale regional geochemical variation along the Mid-Atlantic Ridge (see, for example, White *et al.* 1976) and the geochemical similarity between m.o.r.b. from the Azores platform and alkali basalts in the Azores Islands (White 1977; Schilling 1978). Supporting evidence also comes from D.S.D.P. samples from the same latitude but of different ages (see, for example, Wood *et al.* 1979). They show long-term and large-scale regional geochemical characteristics.

In terms of the model of a chemically stratified mantle, m.o.r.b. and ocean island basalts could come from different layers. In this case, heterogeneity must also exist within each layer, because simple mixing of two components is not adequate to explain the isotopic data (see figure 19).

(b) Generation of linear regression lines on Pb isotopic ratio plots

The fact that volcanic leads from oceanic and island arc environments plot to the right of the Geochron and form linear trends (figures 9 and 10) demonstrates that a single-stage closed-system evolution model is not satisfactory. Mantle processes such as core formation, influx of meteoritic material after core formation, multi-stage evolution, secular increase of U/Pb ratio, mantle mixing and continuous input of crustal radiogenic Pb are necessary.

There are several ways of generating linear regression lines on Pb isotopic ratio plots: closed system multi-stage evolution with random variation of $\mu(^{238}\text{U}/^{204}\text{Pb})$ values; continuous increase of μ imposed on the multi-stage evolution; two-stage episodic mantle differentiation (see, for example, Kanasewich 1962; Cooper & Richards 1966; Oversby & Gast 1970); mixing of two mantle components (see, for example, Sun *et al.* 1975); continuous mantle-crust mixing (Armstrong 1968; Armstrong & Hein 1973); magma chamber contamination (Oversby & Gast 1970; Tatsumoto 1978).

Evolution of Pb isotopic composition with time can be expressed by the following set of equations:

$$({}^{206}\text{Pb}/{}^{204}\text{Pb})_{\text{obs}} = ({}^{206}\text{Pb}/{}^{204}\text{Pb})_{T_0} + \int_0^{T_0} \mu(t) e^{\lambda_8 t} \lambda_8 dt,$$

$$({}^{207}\text{Pb}/{}^{204}\text{Pb})_{\text{obs}} = ({}^{207}\text{Pb}/{}^{204}\text{Pb})_{T_0} + \frac{1}{137.88} \int_0^{T_0} \mu(t) e^{\lambda_5 t} \lambda_5 dt,$$

$$({}^{208}\text{Pb}/{}^{204}\text{Pb})_{\text{obs}} = ({}^{208}\text{Pb}/{}^{204}\text{Pb})_{T_0} + \int_0^{T_0} \mu(t) K(t) e^{\lambda_2 t} \lambda_2 dt,$$

where $\mu = {}^{238}\text{U}/{}^{204}\text{Pb}$, $K = {}^{232}\text{Th}/{}^{238}\text{U}$, $\lambda_8 = 0.155125 \text{ Ga}^{-1}$, $\lambda_5 = 0.98485 \text{ Ga}^{-1}$, $\lambda_2 = 0.049475 \text{ Ga}^{-1}$.

On plot of ${}^{207}\text{Pb}/{}^{204}\text{Pb}$ against ${}^{206}\text{Pb}/{}^{204}\text{Pb}$, the slope for a closed-system multi-stage evolution model with random variation of μ is determined by the timing of the first differentiation event t_1 : $\Delta^{207}\text{Pb}/\Delta^{206}\text{Pb} = (e^{\lambda_5 t_1} - 1)/137.88 (e^{\lambda_8 t_1} - 1)$; if a later event with a large range of variation in μ is superimposed on earlier stages with a small range of variation then the slope is determined by the timing of the later event. This situation could be considered as a 'modified' two-stage model. In a broad sense, the two-stage model allows a previous history of heterogeneity which could be diminished by a homogenization process before the start of the episodic event; in terms of the model with continuous increase of μ (open system), the regression line will have a $\Delta^{207}\text{Pb}/\Delta^{206}\text{Pb}$ slope indicating a t_1 age younger than the time of the start of differentiation (see, for example, Cooper & Richards 1966); in terms of the two-mantle component mixing model, the slope does not necessarily have an age significance; in terms of the mantle-crust mixing model, the $\Delta^{207}\text{Pb}/\Delta^{206}\text{Pb}$ slope will be determined by the composition of the crustal and mantle Pb, their relative contribution and the frequency of mixing (Armstrong 1968; Armstrong & Hein 1973). This model could be modified to include mixing of mantle components (Armstrong & Hein 1973) and open-system evolution (Rennick 1973).

It is a challenging task to justify the choice of a specific model in data interpretation. Frequently, it depends on other geochemical, geological and geophysical information. For example, Sun *et al.* (1975) adopted the two-component mixing model for Iceland–Reykjanes ridge Pb data because it could also explain other geochemical data from this area. On the other hand, to interpret the general $\Delta^{207}\text{Pb}/\Delta^{206}\text{Pb}$ slope of about 0.10 for ocean island Pb, Sun & Hanson (1975*a*) adopted the modified two-stage model because Rb–Sr isotope systematics also appear to give a similar model age (*ca.* 2 Ga). For island arc Pb, the choice of the mantle–crust mixing model is mainly based on the lithosphere subduction model. It has been frequently pointed out that these choices are not necessarily the unique solutions. Further evaluation of specific models will be presented in the following sections.

(c) Evaluation of mixing model for oceanic Pb

Based on a study of Iceland–Reykjanes ridge samples, Sun *et al.* (1975) and Sun & Jahn (1975) suggested that many of the linear trends on Pb isotopic ratio plots for ocean islands could be produced by a mixing of 'plume' and low-velocity zone (l.v.z.) components. This interpretation was retracted in a later paper by Sun & Hanson (1975*a*). They pointed out that mixing trends are not observed on a plot of ${}^{206}\text{Pb}/{}^{204}\text{Pb}$ against ${}^{87}\text{Sr}/{}^{86}\text{Sr}$. However, one might argue that since only a few Pb and Sr isotope data are available on the same samples, the box presentation in figure 19 is likely to be incorrect. Furthermore, analytical uncertainty, alteration and/or

crustal contamination might have obscured the picture. Consequently the mantle mixing model has to be reconsidered.

Recently, Tatsumoto (1978) interpreted Pb isotopic data from the Hawaiian islands in terms of a plume–lithosphere mixing model. His interpretation is based on the observation that Hawaiian data lie on the same regression line as m.o.r.b. on a plot of $^{207}\text{Pb}/^{204}\text{Pb}$ against $^{206}\text{Pb}/^{204}\text{Pb}$ (figure 15) and intersect the m.o.r.b. field on a plot of $^{208}\text{Pb}/^{204}\text{Pb}$ against $^{206}\text{Pb}/^{204}\text{Pb}$ at the higher $^{206}\text{Pb}/^{204}\text{Pb}$ end (figure 16). He suggested that progressive reaction of the plume component with the lithosphere generates time dependent trends observed in Hualalai–Mauna Loa and Kohala–Mauna Kea–Kilauea volcanoes. As shown in figure 15, there is a positive correlation between $^{206}\text{Pb}/^{204}\text{Pb}$ and $\delta^{143}\text{Nd}/^{144}\text{Nd}$ values† for these volcanoes. This correlation lends further support to the mixing interpretation. Correlation among Pb, Sr and

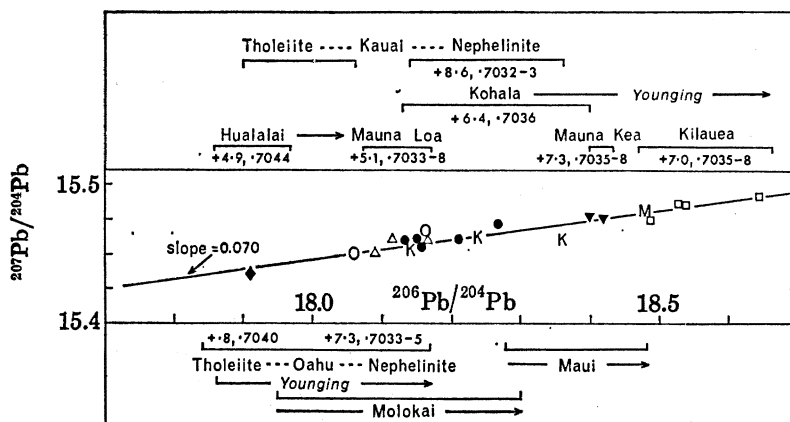


FIGURE 15. Relation between $^{207}\text{Pb}/^{204}\text{Pb}$, $^{206}\text{Pb}/^{204}\text{Pb}$, $^{87}\text{Sr}/^{86}\text{Sr}$ and $\delta^{143}\text{Nd}/^{144}\text{Nd}$ values of Hawaiian volcanics. Data sources are Cooper & Richards (1966), Tatsumoto (1972, personal communication 1978), O'Nions *et al.* (1977), De Paolo & Wasserburg (1976) and this study. Tholeiite: \blacklozenge , Hualalai; \triangle , Mauna Loa; ∇ , Mauna Kea; \square , Kilauea; \bullet , Kohala. Nephelinite: O, Oahu; K, Kauai; M, Maui. +7.3, .7035–8; $\delta^{143}\text{Nd}/^{144}\text{Nd}$, $^{87}\text{Sr}/^{86}\text{Sr}$ range.

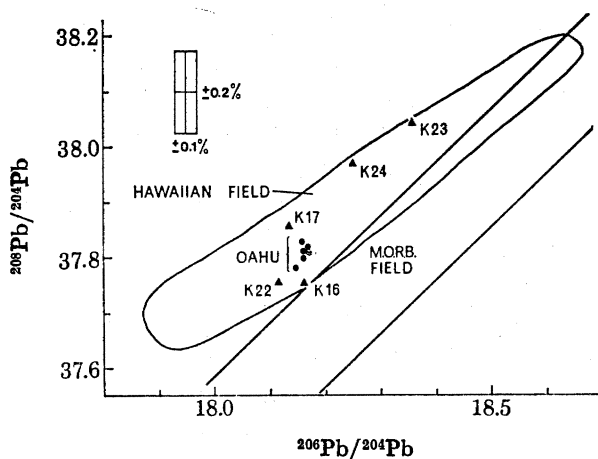


FIGURE 16. Relation of Hawaiian volcanics and m.o.r.b. on a plot of $^{208}\text{Pb}/^{204}\text{Pb}$ against $^{206}\text{Pb}/^{204}\text{Pb}$.

† $\delta^{143}\text{Nd}/^{144}\text{Nd}$ is defined as $\left[\frac{(^{143}\text{Nd}/^{144}\text{Nd})_{\text{sample}}}{(^{143}\text{Nd}/^{144}\text{Nd})_{\text{Juv.}}} - 1 \right] \times 10^4$. Juv. stands for Juvinas achondrite (Lugmair *et al.* 1976).

Nd isotopic data of tholeiites and nephelinites from Oahu and Kauai could also be interpreted in terms of the plume–lithosphere (or preferably l.v.z.) mixing model. The plume component presumably had $^{206}\text{Pb}/^{204}\text{Pb} \approx 17.8$ and $^{87}\text{Sr}/^{86}\text{Sr} \approx 0.7045$.

It is interesting to note that Pb isotopic compositions of tholeiites from Hawaii cover the total range observed in the Hawaiian islands chain (figure 15). Samples from the Hawaiian islands also have the tendency to become more radiogenic in Pb with decreasing age. Tholeiites from the western islands (Kauai and Oahu) have less radiogenic Pb than the eastern islands (Molokai and Maui).

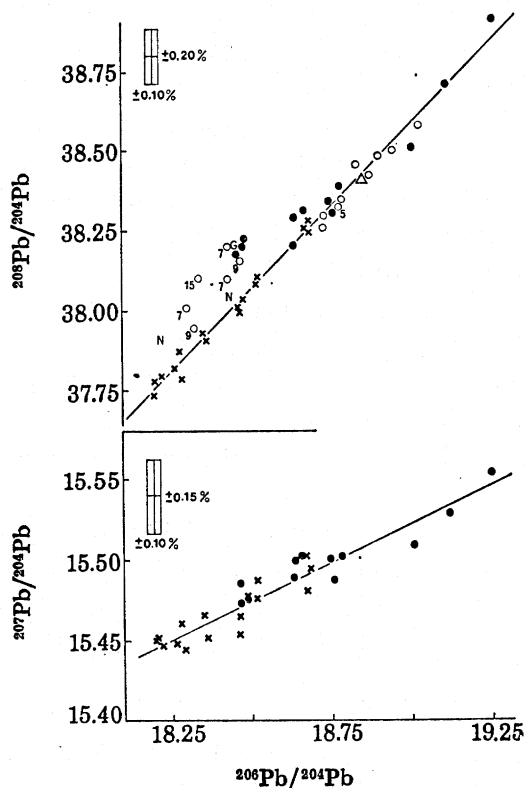


FIGURE 17. Results for samples from Iceland and Reykjanes ridge. Data of Welke *et al.* (1968) (Δ , Surtsey, 1966; \circ , Iceland, 7 Ma; \square , Galena, *ca.* 10 Ma; N , N Iceland, Myvatn) are also presented on a plot of $^{208}\text{Pb}/^{204}\text{Pb}$ against $^{206}\text{Pb}/^{204}\text{Pb}$ after normalization (see text). \bullet , Sun & Jahn (1975), post-glacial S Iceland; \times , Sun *et al.* (1975), Reykjanes Ridge.

A shortcoming of this two-component mixing model is the lack of full range correlation among Pb, Sr and Nd isotopic data. There is no continuous decrease of $^{87}\text{Sr}/^{86}\text{Sr}$ and increase of $\delta^{143}\text{Nd}/^{144}\text{Nd}$ towards the m.o.r.b.-type component. The nephelinites have lower radiogenic Pb and Sr but more radiogenic Nd isotopes than the Kilauean samples, which are presumably close to the m.o.r.b.-type component. Furthermore, Kilauean samples have $^{87}\text{Sr}/^{86}\text{Sr}$ (0.7035–0.7038) much higher than typical m.o.r.b. (*ca.* 0.7027).

It follows that if the plume–lithosphere (or l.v.z.) mixing model for Hawaiian volcanics is correct, then more than two components are necessary. This could imply heterogeneity in the lithosphere or l.v.z. beneath the Hawaiian chain and/or crustal contamination by sea water reaction products such as zeolites (Condomines *et al.* 1976), which could raise Sr isotopic ratios in the tholeiites.

One important implication of this mixing model is on the genesis of Hawaiian nephelinitic magmas. Pb, Sr and Nd isotopic data of nephelinites from Oahu and Kauai require increased involvement of the depleted l.v.z. component than their underlying tholeiites. These nephelinites have light r.e.e. highly enriched patterns and are also enriched in other incompatible elements. In contrast, the underlying tholeiites are only slightly enriched in light r.e.e. It follows that the enrichment in nephelinites must be generated in a very recent time (within a few megayears) in the l.v.z. probably through a zone-refining process (Kay 1975).

Another case of possible two mantle component mixing occurs in the Iceland–Reykjanes ridge system. On the plot of $^{207}\text{Pb}/^{204}\text{Pb}$ against $^{206}\text{Pb}/^{204}\text{Pb}$ (figure 17), data (Sun & Jahn 1975; Sun *et al.* 1975) fall on a linear trend, giving a slope of 0.095 ± 0.006 (1σ). On the plot of $^{208}\text{Pb}/^{204}\text{Pb}$ against $^{206}\text{Pb}/^{204}\text{Pb}$, the situation is similar to that for Hawaiian, i.e. those Icelandic samples with the same $^{206}\text{Pb}/^{204}\text{Pb}$ (*ca.* 18.5) as Reykjanes ridge samples appear to have higher $^{208}\text{Pb}/^{204}\text{Pb}$ ratios. Data from Welke *et al.* (1968) are also shown on this plot. Mass fractionation correction for these data (0.2–0.3% per atomic mass unit) are obtained by assuming that after correction their data will also plot on the $\Delta^{207}\text{Pb}/\Delta^{206}\text{Pb}$ regression line (figure 17), which is defined by more accurate data. Because of this uncertainty, the above conclusion can only be taken as tentative. A reanalysis of samples used by Welke *et al.* (1968) is planned.

In addition to Pb isotopic data, $^{87}\text{Sr}/^{86}\text{Sr}$ (*ca.* 0.7035) and $\delta^{143}\text{Nd}/^{144}\text{Nd}$ (*ca.* +6) data (O’Nions & Pankhurst 1973; O’Nions *et al.* 1977) on Tertiary Icelandic samples (with $^{206}\text{Pb}/^{204}\text{Pb} < 18.5$) also indicate that they are different from Reykjanes ridge m.o.r.b. with similar Pb isotopic composition. The Reykjanes ridge samples have $^{87}\text{Sr}/^{86}\text{Sr} \approx 0.7028$ and expected $\delta^{143}\text{Nd}/^{144}\text{Nd} \approx +10$.

Another case of possible two mantle component mixing comes from 45° N Mid-Atlantic Ridge. Pb, Sr isotopic and trace element data from this area (Sun *et al.* 1980) appear to satisfy the mixing model. Pb isotopic data fall between the fields of Azores and normal m.o.r.b. There is a positive correlation between Pb, Sr isotopic ratios and $(\text{La}/\text{Sm})_{\text{N}}$ ratio.

(d) Model ages for oceanic Pb

Linear regression of Pb isotopic data gives a $\Delta^{207}\text{Pb}/\Delta^{206}\text{Pb}$ slope of 0.104 ± 0.007 (1σ) for the Canary Islands; 0.095 ± 0.006 for the Iceland–Reykjanes ridge; 0.090 ± 0.010 for Iceland; 0.121 ± 0.009 for the Juan de Fuca–Gorda ridges and associated seamounts (50 samples) and 0.112 ± 0.011 for NE Pacific seamounts alone (21 samples; Church & Tatsumoto 1975).

In terms of the two-stage model, the slopes will correspond to ages of 1.70 ± 0.12 (1σ) Ga for the Canary Islands, 1.5 ± 0.25 Ga for Iceland, and 1.84 ± 0.18 Ga for NE Pacific seamounts. Church & Tatsumoto (1975) have reported a more accurate value of 1.75 ± 0.1 Ga for the NE Pacific seamounts by averaging two regression lines derived from the same set of data. However, this practice is not justified.

If the two-stage model (or multi-stage random mixing) is applicable, it suggests that a major mantle differentiation event took place *ca.* 1.7 Ga ago in the mantle sources for Canary Island volcanics. Sun & Hanson (1975*a*) suggest that two stage model age of *ca.* 2.0 Ga shown by most ocean island Pb (figure 9) might represent the time when large-scale mantle convective mixing processes slowed down and preservation of isotopic heterogeneity over long periods of time became common.

The two-stage model age for Gough–Discovery Tablemount (and probably Tristan da Cunha) is very small (not more than a few megayears). It suggests that their mantle sources

have been in homogeneous system until recently. $^{87}\text{Sr}/^{86}\text{Sr}$ ratios for Gough, Discovery Tablemount and Tristan da Cunha samples are about 0.705 (O'Nions & Pankhurst 1974; Gast *et al.* 1964; Sun, unpublished data) and $^{143}\text{Nd}/^{144}\text{Nd}$ ratios for Tristan da Cunha samples (O'Nions *et al.* 1977) are close to chondritic. Isotopic data (Pb, Sr and Nd) on these samples seem to suggest that they are from the least disturbed mantle domains in the oceanic environment.

A drawback to the simple two-stage model comes from other geochemical observations. There are now abundant data to suggest that the mantle sources for oceanic alkali basalts and 'plume' type m.o.r.b. are enriched in incompatible elements (see, for example, Sun & Hanson 1975*b*; White 1977; Sun *et al.* 1979). Available Nd and Sr isotope data on these samples (see, for example, De Paolo & Wasserburg 1976; O'Nions *et al.* 1977; Carlson *et al.* 1978; Sun *et al.* 1979) would limit timing of the enrichment process to comparatively recent times (less than a few hundred megayears).

In terms of the mantle differentiation model with continuous increase of μ value and random redistribution, the starting time of mantle differentiation is greater than that indicated by the two-stage model (see, for example, Cooper & Richards 1966). For example, the observed mantle heterogeneity might have started at the late Archaean (*ca.* 2.7 Ga) when effective mantle convection gradually slowed down. An increase in μ with time could be achieved by upward enrichment of U by migration of a fluid phase or silicate melt or by downward segregation of Pb by a sulphide phase. Further discussion of this problem will be presented in §5*h*.

(e) *Mantle-crust mixing model*

Considering the consequence of lithosphere subduction, Armstrong (1968) constructed a steady-state mantle-crust continuous mixing model to explain Pb and Sr isotopic data from the continental and oceanic environments. A basic concept of Armstrong's model is that there was an early worldwide depletion of incompatible elements in the upper mantle which was caused by formation of proto-continental crust. Introduction of continental sediments has kept Pb and Sr isotopes in the upper mantle 'alive'. A major objection to this model comes from trace elements (see, for example, Sun & Nesbitt 1977), Sr isotopes (see, for example, Jahn & Nyquist 1976) and Nd isotopic data (e.g. those of De Paolo & Wasserburg 1976; Hamilton *et al.* 1977; Zindler *et al.* 1978; McCulloch & Wasserburg 1978). These data suggest that magma sources in the late Archaean (*ca.* 2.7 Ga) mantle were either undepleted or much less depleted than sources for modern m.o.r.b. It follows that development of depletion in the m.o.r.b. source is a post-Archaean process and was possibly started by the greenstone belt-forming event 2.7 Ga ago. Repeated occurrences of fertile tholeiites throughout post-Archaean time in various parts of the world clearly suggest that depletion did not take place throughout the entire mantle in the Archaean.

A further objection comes from correlation patterns between Pb and Sr ratios of ocean volcanics. As shown in figure 19, there is a tendency for samples with very radiogenic Pb to have the least radiogenic Sr. This is contrary to expectations from the mantle-crust mixing model.

It is possible that crustal input does affect the isotopic evolution in the mantle to a certain extent. However, it is difficult to quantify it at present.

(f) *Involvement of crustal material in island arc magma genesis*

There is no general consensus on the interpretation of the apparent crust-mantle Pb mixing trends for island arc volcanics. Although the effect of crustal contamination is well demonstrated

in many instances of continental volcanism (see, for example, Armstrong *et al.* 1977; Chen & Tilton 1978), a straightforward crustal contamination model is not applicable to island arcs built on the oceanic crust. In this case, Kay *et al.* (1978) suggested that the crustal component in the volcanic Pb could come from two possible sources: (a) the clastic wedge associated with the initial underthrusting onto which the island arc was built and/or (b) sediments trapped in fractures (due to lithosphere bending) in the currently underthrusting oceanic plate. A geological

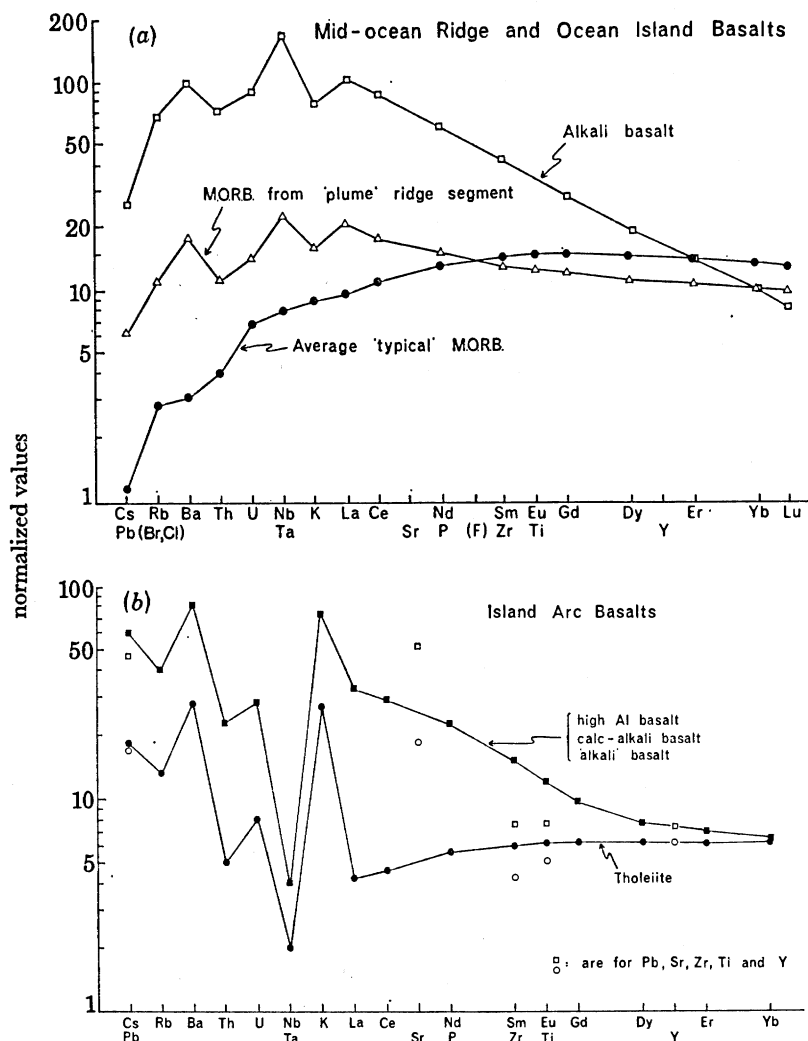


FIGURE 18. Comparison of normalized abundance patterns of incompatible elements in basalt from oceanic islands, oceanic ridges and island arcs. Normalizing values are presented in table 9. For refractory lithophile elements such as Ti, Zr, r.e.e., U and Th, chondritic values are used. Normalizing value for Pb is derived by assuming $^{238}\text{U}/^{204}\text{Pb} \approx 8.0$ for 'undepleted' Earth mantle. Normalizing values for Cl, Br and F are estimated as 10, 0.03 and 13 $\mu\text{g/g}$ respectively based on data in the literature (e.g. Schilling 1978).

observation in favour of subduction of sediments is the existence of high P /low T metamorphic belts along the subduction zone, which indicates underthrusting of sediment wedge to great depth. The degree of involvement of a crustal component depends on the accessibility to the sediment source and probably also on the ageing of the island arc.

Within the plate tectonic framework, magma generation at an island arc could involve three components, i.e. mantle wedge above the subduction zone, subducted oceanic crust plus clastic sediments, and crustal material near the surface. Ringwood (1974) points out that the geochemical characteristics of island arc volcanics could be influenced by different magma generation processes underneath the island arc, by the residual mineralogy and by introduction of supercritical solutions or silicate melts from the subducted lithosphere into the mantle wedge above. The relative importance of each component and processes could be evaluated by using available trace element and Pb and Sr isotopic data.

TABLE 9. TRACE ELEMENT ABUNDANCES (micrograms per gram) IN REPRESENTATIVE SAMPLES†
FROM MID-OCEAN RIDGES, OCEAN ISLANDS AND ISLAND ARCS

	Cs	Pb	Rb	Ba	Th	U	Ta	Nb	K
m.o.r.b.									
depleted	0.013	0.40	1.0	12	0.20	0.10	0.16	3.1	1060
enriched	0.076	0.66	3.9	68	0.55	0.18	0.46	8.1	1920
ocean island									
alkali basalt	0.31	2.9	22	380	3.4	1.1	3.0	53	9600
island arc									
tholeiite	0.22	1.9	4.6	110	0.25	0.10	—	0.7	3240
high Al-basalt	0.72	5.6	14	300	1.1	0.36	—	1.4	8640
calc-alkali basalt									
'alkali' basalt									
normalizing values‡	0.012	0.12	0.35	3.8	0.050	0.013	0.020	0.35	120
	La	Ce	Sr	Nd	P	Sm	Zr	Ti	Y
m.o.r.b.									
depleted	3.0	9.0	124	7.7	600	2.8	85	9300	29
enriched	6.3	15	180	9.0	690	2.5	75	8060	22
ocean island									
alkali basalt	35	72	800	35	2760	13	220	20000	30
island arc									
tholeiite	1.3	3.7	200	3.4	—	1.2	22	3000	12
high Al-basalt	10	23	550	13	—	2.9	40	4650	15
calc-alkali basalt									
'alkali' basalt									
normalizing values‡	0.315	0.813	11	0.597	46	0.192	5.6	620	2.0

† Data are based on least fractionated samples. A range of absolute abundance does exist within each rock group and only relative patterns (figure 18*a, b*) are emphasized. Major references: Erlank & Kable (1976), Ewart *et al.* (1977), Church & Tatsumoto (1975), Hart (1976), Kay & Hubbard (1978), White (1977), Gorton (1977), Sun *et al.* (1979) and this study.

‡ Based on chondrite data and the composition of 'undepleted' model mantle. For details, see Sun *et al.* (1979).

Figures 18*a, b* and table 9 present a comparison of trace element abundance patterns between island arc and ocean volcanics. The abundance patterns in figure 18*b* represent island arc samples from both continental margins (e.g. Japan and eastern Aleutian islands) and from oceanic environments (e.g. Tonga, Scotia arc, New Hebrides, New Britain, Mariana, etc.). It is quite clear that, relative to m.o.r.b. and ocean island basalts, volcanic rocks from island arcs have an over-abundance of Sr, K, Th, U, Ba, Rb, Cs and Pb and an under-abundance of Ti, Zr, Nb and Ta.

Since Pb isotopic compositions of volcanic rocks from Tonga (figure 14), New Hebrides (Lancelot *et al.* 1978) and the Mariana Arc (Meijer 1976) are very similar to m.o.r.b.,

over-abundance of Pb and other trace elements in these volcanics (Ewart *et al.* 1977; Hart & Brooks 1977; Meijer *et al.* 1978; Gorton 1977) cannot be due to involvement of sediments. Samples from these oceanic type island arcs (also Scotia arc) have $^{87}\text{Sr}/^{86}\text{Sr}$ ratios not less than 0.7035, which is considerably higher than m.o.r.b. with a similar r.e.e. pattern and Nd isotopic ratios (see, for example, Hawkesworth *et al.* 1978; Hart & Brooks 1977). The over-abundant Pb, Sr and other trace elements are most likely derived from dehydration or partial melting of the subducted-altered oceanic crust. Fluid phase or wet silicate melt transportation above the subduction zone might also be important. Direct remelting of the oceanic crust to generate the island arc tholeiites is not a viable mechanism (see, for example, Arth 1974) because P - T conditions of the Benioff Zone under the tholeiitic volcanics are generally within eclogite facies (see, for example, Ringwood 1974). Partial melting of the subducted oceanic crust will generate melts with highly fractionated r.e.e. patterns showing severe depletion in heavy r.e.e. (see, for example, Ringwood 1974; Kay 1978).

In Japanese tholeiites with light r.e. depleted patterns and Pb isotopic compositions halfway between sediment and m.o.r.b. components, the degree of possible sediment contribution to trace element over-abundances could also be estimated in a way similar to estimates made by Tatsumoto (1969) and Armstrong (1971). Let us assume that the 'uncontaminated' sub-island arc mantle has trace element abundances (all in micrograms per gram) similar to m.o.r.b. sources (table 9) with Pb = 0.10, Th = 0.05, U = 0.025, Ba = 3, Rb = 0.25, Sr = 30, K = 270 and $^{87}\text{Sr}/^{86}\text{Sr} = 0.7027$, and that the clastic sediments have Pb = 20, Th = 10, U = 2.5, Ba = 1000, Rb = 100, Sr = 200, K = 3.0% and $^{87}\text{Sr}/^{86}\text{Sr} = 0.710$ (see, for example, Church 1973). A simple two-component mixing calculation suggests that 0.5% sediment assimilation can produce the observed Pb isotopic composition and generate some degree of over-abundance in Sr (3%), Ba and Rb (200%), Th and Pb (100%), U (50%), K (60%) and cause a 0.00025 increase in $^{87}\text{Sr}/^{86}\text{Sr}$ ratio. This contribution only explains a small portion of the observed trace element over-abundance (compare figure 18*a* and *b*) and high $^{87}\text{Sr}/^{86}\text{Sr}$ ratios (*ca.* 0.7035) in Japanese tholeiites (see, for example, Tatsumoto & Knight 1969; Philpotts *et al.* 1971; Hart & Brooks 1977). If the elemental over-abundance is mainly due to contribution from the subducted oceanic crust and sediment (see, for example, Tatsumoto 1969; Armstrong 1971), about 2% sediment will be required to keep Pb isotopic composition in balance. The resultant over-abundance of Ba and Rb (and Cs) will be strongly controlled by the sediment as well as subducted altered m.o.r.b., while Sr and $^{87}\text{Sr}/^{86}\text{Sr}$ will be mainly affected by the subducted 'altered' m.o.r.b.

This kind of calculation can be carried further. If an island arc basalt has 75% Pb isotopic component from sediment, then the increase in $^{87}\text{Sr}/^{86}\text{Sr}$ will be 0.00075 (e.g. an increase from 0.7027 to 0.7035). A shortcoming of these calculations is that they can be complicated by selective leaching of the subducted sediment and m.o.r.b. and by elemental fractionation during partial melting. For example sphene (U-rich, Th-poor) and amphibole (Th-rich, U-poor) are possible residual minerals beneath an island arc. They could cause significant fractionation of Th and U.

It is obvious that the subducted clastic sediment could be a very important source for Cs, Ba, Rb, Pb, Th and U in the island arc volcanics. However, it is not clear how much of the subducted sediment components remain unconsumed at the island arc magma generation site and are later recycled into other parts of the mantle to affect Pb and Sr isotopic evolution within it.

(g) Variation of U/Pb and Th/U ratios in the Earth's mantle

The behaviour of U, Th and Pb during mantle partial melting is not yet well understood (Tatsumoto 1978). The chalcophile affinity of Pb and the possible existence of sulphide melt in the mantle further complicate the situation. Post-magmatic deuteric alteration can also change their abundances in the volcanic rocks. For example, among m.o.r.b. from Juan de Fuca–Gorda Ridges with very similar Pb isotopic composition (Church & Tatsumoto 1975), there is more than a two-fold variation in U/Pb and Th/U ratios. These variations must be due to very recent processes.

It has been suggested that during generation of alkali basalts and nephelinites magmas could have μ higher by a factor of two to three than the source because of lower mineral-melt K_d for U than Pb, and existence of sulphide melt (Gast 1969; Tatsumoto 1978; Sun & Hanson 1975*b*). Partial melting processes may also have increased Th/U in the magma. For example, samples from the Canary Islands have measured Th/U ratios averaging 4.0 (Oversby 1969; this study), while the inferred source ratio based on $^{230}\text{Th}/^{238}\text{U}$ activity is about 20% lower (Oversby 1969). A similar situation has also been found in samples from Tristan da Cunha, where the measured Th/U ratio averages 4.2 and the inferred source ratio is about 3.7 (Oversby & Gast 1968). If this $^{230}\text{Th}/^{238}\text{U}$ method is correct and generally applicable, then the measured Th/U ratio in alkali basalts and nephelinites (Tatsumoto 1966*a, b*; Oversby 1969; Zartman & Tera 1973; this study) from St Helena (*ca.* 3.5), Canary Island (*ca.* 4.0), Guadalupe (*ca.* 3.7) and the Hawaiian islands (*ca.* 3.5) would suggest that their sources have a Th/U ratio (3.0–3.5) too low to support long-term radiogenic growth of ^{208}Pb . Decrease of the Th/U ratio in more recent time (less than 1 Ga) is suggested. Alternatively it could also be due to a gradual decrease of Th/U ratio through time.

Typical m.o.r.b. have Th/U ratios averaging 2.0, which is far less than the value of *ca.* 3.7 required for radiogenic growth of ^{208}Pb . This is a major point in Armstrong's (1968) mantle-crust mixing model. He suggests that continuous input of crustal Pb has sustained ^{208}Pb growth. On the other hand, Tatsumoto (1978) suggests that Pb isotopic composition of m.o.r.b. could be explained by increase of Th/U ratio from 3.8–4.0 (primitive Earth) to 4.2–4.5 during mantle-protocrust differentiation in the early Earth history and then gradual decrease through geological time in the m.o.r.b. source.

It is interesting to notice that samples from Tristan da Cunha and Gough Island have measured (*ca.* 4.2) and inferred (*ca.* 3.7) Th/U ratios close to that required (*ca.* 4.0) for a closed-system evolution. These samples also have $^{87}\text{Sr}/^{86}\text{Sr}$ (*ca.* 0.7050) and $^{143}\text{Nd}/^{144}\text{Nd}$ (for Tristan da Cunha) close to that estimated for primitive Earth mantle (e.g. by De Paolo & Wasserburg 1976; O'Nions *et al.* 1977).

(h) Correlation among Pb, Sr and Nd isotopic data from ocean environments

It has been established that there is an inverse correlation between $^{87}\text{Sr}/^{86}\text{Sr}$ and $^{143}\text{Nd}/^{144}\text{Nd}$ ratios of volcanic rocks from the oceanic environment (e.g. by De Paolo & Wasserburg 1976; O'Nions *et al.* 1977). This relation could be interpreted as an indication of coherency between Rb/Sr and Nd/Sm ratios in the mantle and could be a result of transfer of silicate melt or fluid phase in the mantle. In contrast, the relation between Pb and Sr isotopic ratios of ocean volcanics is more complicated. As shown in figure 19, no clear trend can be demonstrated.

Based on an earlier version of the plot of $^{206}\text{Pb}/^{204}\text{Pb}$ against $^{87}\text{Sr}/^{86}\text{Sr}$ by Sun & Hanson

(1975*a*) and their own data from Kerguelen, Vidal & Dosso (1978) have recently emphasized the rough inverse correlation trend in this plot, with Hawaiian data as an exception. They suggest that this trend could be generated by separation of a sulphide phase into the core and the apparent mantle Pb isochron age of *ca.* 2.0 Ga could represent the closing time of core formation.

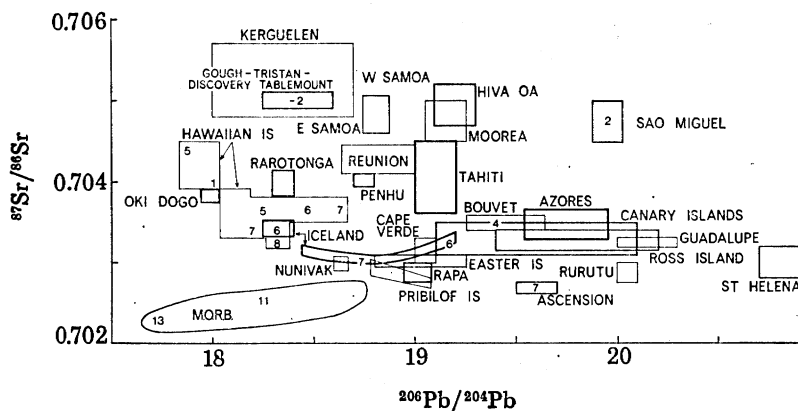


FIGURE 19. Relation between $^{206}\text{Pb}/^{204}\text{Pb}$ and $^{87}\text{Sr}/^{86}\text{Sr}$ ratios of oceanic island volcanics. $\delta^{143}\text{Nd}/^{144}\text{Nd}$ values are also presented as numerical values in the boxes. This plot is a modified version of that of Sun & Hanson (1975*a*). Additional data sources include Batiza (1977), De Paolo & Wasserburg (1976), Dosso (1977), Duncan & Compston (1976), Dupré *et al.* (1978), Hawkesworth *et al.* (1978), Kay *et al.* (1978), O'Nions *et al.* (1977), Sun (unpublished data), White *et al.* (1976) and this study.

The thrust of their model hinges on the assumed behaviour of a sulphide phase which is believed to concentrate alkali elements (K, Rb) in addition to Pb. If so, separation of a sulphide phase will simultaneously cause a significant increase of U/Pb and decrease of Rb/Sr ratios in the mantle system, and the inverse correlation between Pb and Sr isotopic ratios can then be generated. However, this alleged separation of most mantle Rb into the core is not supported by available cosmochemical and geochemical data. For example, Wasson & Chou (1974) show that depletion of moderately volatile elements such as K, Rb, Na and Mn in ordinary chondrites relative to C1 chondrites is about the same. An estimate for primitive Earth mantle by Sun & Nesbitt (1977) indicates only limited relative fractionation among these elements relative to C1 chondrites, i.e. Na = 0.19, Mn = 0.21, Rb = 0.13 and K = 0.16. Since neither Mn nor Na will concentrate into an iron or sulphide phase, these data are not consistent with the idea that most (more than 40%) of the Earth's Rb is stored in the core. Initial $^{87}\text{Sr}/^{86}\text{Sr}$ isotopic ratios from Archaean greenstone belts also support this argument. Komatiites and barites from the 3.5 Ga Barberton Mountainland, S Africa (Jahn & Nyquist 1976), and barite from *ca.* 3.5 Ga Pilbara, Australia (S. S. Goldich, personal communication 1974) give initial $^{87}\text{Sr}/^{86}\text{Sr}$ ratios *ca.* 0.7005 and most 2.7 Ga greenstone belts from various parts of the world give initial $^{87}\text{Sr}/^{86}\text{Sr}$ ratios *ca.* 0.7010 (Jahn & Nyquist 1976; Hart & Brooks 1977). These data are consistent with evolution history in a mantle with Rb/Sr *ca.* 0.030. They are not consistent with the idea that in the early history of the Earth's mantle its Rb/Sr ratio was close to that of C1 chondrite (*ca.* 0.25).

Figure 19 presents more data than the earlier version by Sun & Hanson (1975*a*). It is clear that within the range $^{206}\text{Pb}/^{204}\text{Pb} = 18.0\text{--}19.2$, $^{87}\text{Sr}/^{86}\text{Sr}$ ratio varies from 0.703 to 0.705 without a correlation trend. Many 'uncontaminated' alkali and tholeiitic basalts from the

continents also plot within this field (not shown). A distinctive feature of this diagram is that those samples with $^{206}\text{Pb}/^{204}\text{Pb} \geq 19.5$ have low $^{87}\text{Sr}/^{86}\text{Sr}$ ratios (0.7028–0.7035). One exception to this generalization is presented by samples from eastern Sao Miguel, Azores. They have $^{206}\text{Pb}/^{204}\text{Pb} \approx 20.0$ and $^{87}\text{Sr}/^{86}\text{Sr} \approx 0.705$ (Dupré *et al.* 1978; White *et al.* 1976).

Following the above reasoning and observation, it is more likely that low $^{87}\text{Sr}/^{86}\text{Sr}$ in some of the oceanic volcanics is mainly related to the same process, such as upward migration of a fluid or melt phase, which also caused the $^{143}\text{Nd}/^{144}\text{Nd}$ variation. Small degrees of partial melting in the mantle will decrease its viscosity and will create a favourable condition for downward separation of sulphide melt with very low U/Pb ratio. These two processes together might explain better the correlation of high $^{206}\text{Pb}/^{204}\text{Pb}$ with low $^{87}\text{Sr}/^{86}\text{Sr}$ in figure 19. The suggestion (also made by Vidal & Dosso 1978) that high μ in the mantle is generally due to depletion of Pb instead of enrichment of U, is supported by trace element abundance patterns for oceanic basalts (figure 18*b*).

(i) *Development of a heterogeneous mantle*

The issue of the development of a heterogeneous mantle is related to questions concerning the timing, mechanism and nature of the processes which have generated the observed chemical and isotopic heterogeneity in the mantle.

The mantle has experienced disturbances since the early history of the Earth. Processes such as formation of a proto-crust, iron core, partial melting in the mantle and continuous influx of meteoritic material after core formation are expected to create chemical heterogeneity in the mantle. To counterbalance these processes, vigorous mantle convection at that time offers a homogenization mechanism. R.e.e. studies of *ca.* 3.8–3.5 Ga Archaean greenstones from Western Greenland, S Africa, Western Australia and N America (Sun & Nesbitt 1977, 1978, unpublished data; Hanson, personal communication, 1976) and 2.7 Ga greenstones from various parts of the world (Sun & Nesbitt 1977, 1978; Jahn *et al.* 1979; Arth *et al.* 1977) indicate that their mantle sources were considerably heterogeneous. Many of the Archaean basalts are depleted in light r.e.e. but they always have $(\text{La}/\text{Sm})_{\text{N}} \geq 0.70$. In contrast modern m.o.r.b. from normal ridge segments have $(\text{La}/\text{Sm})_{\text{N}} = 0.40\text{--}0.70$. The only Archaean rock type showing severe light r.e.e. depletion similar to modern m.o.r.b. are the high-magnesian ($\text{MgO} = 20\text{--}30\%$) spinifex textured komatiites which most probably were developed by a short term multi-stage melting process during a major magma generation event (see, for example, Sun & Nesbitt 1978; Zindler *et al.* 1978). Available $^{143}\text{Nd}/^{144}\text{Nd}$ isotopic data on 2.7 Ga Rhodesian and Canadian greenstones (including spinifex textured komatiites) and several Archaean granitoids from various parts of the world (Hamilton *et al.* 1977; McCulloch & Wasserburg 1978; Zindler *et al.* 1978) suggest that their sources have evolved in an environment close to chondritic which did not have a long-term light r.e.e. depleted history.

Depletion of incompatible elements in the m.o.r.b. sources, which presumably represent a large part of the Earth's mantle, could be accomplished through an episodic or a continuous mantle evolution. Although there is a possibility that the depletion is caused by the 2.7 Ga greenstone forming event, the low Rb/Sr (*ca.* 0.008) and Th/U (*ca.* 2.0) ratios (presently observed in m.o.r.b.) in the presumed Archaean precursor of m.o.r.b. sources are not enough to generate radiogenic ^{87}Sr and ^{208}Pb observed in m.o.r.b. There is no supporting evidence (Sun *et al.* 1979), either, that depleted m.o.r.b. sources were developed episodically at about 1.6 Ga ago by mantle differentiation into mesosphere and asthenosphere (Brooks *et al.* 1976). On the

other hand, available Pb, Sr and Nd isotopic data do require long-term (more than 1 Ga) depletion of the m.o.r.b. sources. Since there is no positive evidence for either Archaean or Proterozoic events capable of generating the depleted mantle sources for typical m.o.r.b., a continuous evolving mantle would be a favourable alternative. This mantle depletion process could be compensated for by the growth of continental crust. In fact, a gradual decrease of Rb/Sr ratio from 0.03 at 2.7 Ga ago with $^{87}\text{Sr}/^{86}\text{Sr}$ *ca.* 0.7010 to 0.008 at present is capable of generating the radiogenic ^{87}Sr observed in the m.o.r.b. sources. Available Pb and Nd isotopic data on m.o.r.b. were not inconsistent with this interpretation. It is also conceivable that the initial depletion could have started before 2.7 Ga ago.

Major chemical and isotopic heterogeneities observed in the modern oceanic environment are represented by important differences between the mantle sources for ocean island basalts (plus 'plume'-type m.o.r.b.) and typical m.o.r.b. In addition, there are also significant variations within each type of basalts. For example within the typical m.o.r.b. $(\text{La}/\text{Sm})_{\text{N}}$ ratios range from 0.4 to 0.7 and $^{87}\text{Sr}/^{86}\text{Sr}$ ratios vary from 0.7023 to 0.7028. In formulating a mantle evolution model, these differences and variations must be taken into account. The observed variations could be a result of long-term heterogeneity which becomes magnified by short-term processes. For example, the geochemistry of ocean island basalts and plume-type m.o.r.b. (e.g. Azores platform and 45° N M.A.R.) indicate that their mantle sources are enriched in light r.e.e. (Sun & Hanson 1975*b*; White 1977), while other geochemical characteristics such as Sr and Nd isotopes and trace element patterns (figure 18*b*) suggest that they have long-term depleted sources. Plume type m.o.r.b. have considerably higher Rb/Sr ratios than typical m.o.r.b. (0.04 compared with 0.008) but have only slightly higher $^{87}\text{Sr}/^{86}\text{Sr}$ ratios (0.7033 compared with 0.7026). Sun *et al.* (1979) point out that enrichment of Rb and other incompatible elements in the mantle sources for 'plume' m.o.r.b. must be a recent process within a few hundred megayears. Carlson *et al.* (1978) also reach this conclusion, based on a study of Nd isotopes. Supporting argument also comes from Pb isotopic compositions of Hawaiian nephelinites which are considered as a mixing product of less-depleted 'plume' and depleted l.v.z. components (see §5*c*). Large enrichments of incompatible elements in the nephelinite sources must be generated very recently (within a few megayears?) in the l.v.z.

Although Sr and Nd isotopic data of some ocean island basalts and plume-type m.o.r.b. are compatible with the idea that their mantle sources could be derived from more typical m.o.r.b. sources through enrichment processes within the last few hundred megayears, Pb isotopic data (figure 9) are not consistent with such interpretation. For example, if mantle sources for Iceland, St Helena, Ascension, Guadalupe and the Canary Islands and 'plume' m.o.r.b. from 45° N Mid-Atlantic Ridge (Sun *et al.* 1980) are generated from depleted m.o.r.b. sources during the last few hundred megayears, then the regression lines connecting them to the m.o.r.b. field on a plot of $^{207}\text{Pb}/^{204}\text{Pb}$ against $^{206}\text{Pb}/^{204}\text{Pb}$ should be considerably shallower (0.06 and 0.052 corresponding to 600 and 300 Ma respectively) than the generally observed slope of *ca.* 0.10. Therefore Pb isotope data favour a long-term separation between mantle sources for ocean island basalts and m.o.r.b., even if Pb isotopic data could represent mixing of two sources. One possible explanation for the apparent discrepancy between interpretations of Pb, Sr and Nd isotopic data is that mantle sources for ocean islands and typical m.o.r.b. are unrelated and have been isolated from each other for about 2 Ga (see, for example, Sun & Hanson 1975*a*). In this case, Sr and Nd isotopic data could be interpreted differently. For example, enrichment of incompatible elements in the ocean island basalts and plume type m.o.r.b. could be a very recent

process (within a few megayears?) and the observed Sr and Nd isotopic ratios are mainly due to long-term heterogeneity and mantle mixing.

At present the answer to the question of where and how the observed geochemical heterogeneity is generated in the mantle is necessarily speculative. A favourable location is in the low-velocity zone where migration of fluid, silicate or sulphide melt phase is feasible. Possible processes include differentiation of the l.v.z. by migration of fluid or silicate melt towards the top of the l.v.z. (Green 1971; Green & Liebermann 1976), magma extraction, enrichment during mantle diapirism or convection within the l.v.z. or at a later stage at the top of the l.v.z. Mantle mixing could also be involved. It is very likely that the observed heterogeneity is the combined result of several processes. The driving force for these processes lies in the thermal condition of the mantle (and core?) and tectonic processes such as lithosphere subduction.

This paper is an expansion of my Ph.D. thesis work at Columbia University. I was inspired by Armstrong's (1968) paper in which he attempted to synthesize existing Pb and Sr isotopic data and developed a unified mantle-crust dynamic mixing model. I have benefited frequently from his advice. The late Professor P. Gast had given me all the moral support I needed. Dr Virginia Oversby taught me the basic knowledge of Pb isotope analysis. Encouragement and help from Professor W. Broecker were essential to keep my spirits high at the initial stage of this study. I am grateful to Dr and Mrs M. Tatsumoto for their hospitality during my one month visit to Denver, U.S.G.S. Thanks are also due to R.A. Binns, E. Catanzaro, J. A. Cooper, G. N. Hanson, R. Kay, C.-Y. Shih and M. Tatsumoto for their help on various occasions. Dr T. Simkin of the Smithsonian Institution kindly made samples from Tristan da Cunha and Easter Islands available for analysis. Samples from Taiwan were donated by T.-P. Yen, L.-P. Tan, C.-N. Yang and C.-H. Chen. M. Swan and R. Barrett, both at Adelaide University, carefully prepared the figures and prints used in this paper. This research work is supported through fellowships from Columbia University and the Lunar Science Institute.

REFERENCES (Sun)

- Abdel-Monem, A., Watkins, N. D. & Gast, P. W. 1971 *Am. J. Sci.* **271**, 490–521.
 Abdel-Monem, A., Watkins, N. D. & Gast, P. W. 1972 *Am. J. Sci.* **272**, 805–825.
 Almeida, F. 1958 *Monografias Div. geol. miner. Bras.* no. 13, 177 pages.
 Armstrong, R. L. 1968 *Rev. Geophys.* **6**, 175–199.
 Armstrong, R. L. 1971 *Earth planet. Sci. Lett.* **12**, 137–142.
 Armstrong, R. L. & Cooper, J. A. 1971 *Bull. volcan.* **35**, 27–63.
 Armstrong, R. L. & Hein, S. M. 1973 *Geochim. cosmochim. Acta* **37**, 1–18.
 Armstrong, R. L., Taubeneck, W. H. & Hales, P. O. 1977 *Bull. geol. Soc. Am.* **88**, 397–411.
 Arth, J. G. 1974 In *Abstracts, Annual Meeting, Geol. Soc. America*, vol. 6, p. 638.
 Arth, J. G., Arndt, N. T. & Naldrett, A. J. 1977 *Geology* **5**, 590–594.
 Baker, I. 1969 *Bull. geol. Soc. Am.* **80**, 1283–1310.
 Baker, P. E. & Buckley, F. 1974 *Contr. Miner. Petr.* **44**, 85–100.
 Baker, P. E., Gass, I. G., Harris, P. G. & Le Maitre, R. W. 1964 *Phil. Trans. R. Soc. Lond.* A **256**, 439–578.
 Batiza, R. 1977 *Geology*, **5**, 760–764.
 Bell, J. D., Atkins, F. B., Baker, P. E. & Smith, D. G. W. 1967 *Trans. Am. geophys. Un.* **53**, 68.
 Bonatti, E., Harrison, C. G. A., Fisher, D. E., Honnorez, J., Schilling, J.-G., Stipp, J. J. & Zentilli, M. 1977 *J. geophys. Res.* **82**, 2457–2478.
 Brooks, C., Hart, S. R., Hofmann, A. & James, D. E. 1976 *Earth planet. Sci. Lett.* **32**, 51–61.
 Carlson, R. W., Macdougall, J. D. & Lugmair, G. W. 1978 *Geophys. Res. Lett.* **5**, 229–232.
 Catanzaro, E. J. 1967 *Earth planet. Sci. Lett.* **3**, 343–346.
 Chen, J.-C. 1973 *Proc. geol. Soc. China* **16**, 23–36.
 Chen, J. H. & Tilton, G. R. 1978 *Abstr. geol. Soc. Am.* **10**, 100.

- Church, S. E. 1973 *Contr. Miner. Petr.* **39**, 17–32.
- Church, S. E. 1976 *Earth planet. Sci. Lett.* **29**, 175–188.
- Church, S. E. & Tatsumoto, M. 1975 *Contr. Miner. Petr.* **53**, 253–279.
- Chow, T. J. & Patterson, C. C. 1962 *Geochim. cosmochim. Acta* **26**, 263–308.
- Compston, W. & Oversby, V. M. 1969 *J. geophys. Res.* **74**, 4338–4348.
- Condomines, M., Bernat, M. & Allègre, C. J. 1976 *Earth planet. Sci. Lett.* **33**, 122–125.
- Cooper, J. A. & Richards, J. R. 1966 *Earth planet. Sci. Lett.* **1**, 259–269.
- Daly, R. A. 1925 *Proc. Am. Acad. Arts. Sci.* **60**, 1–124.
- Daly, R. A. 1927 *Proc. Am. Acad. Arts. Sci.* **62** (2).
- DeLong, S. E., Hodges, F. N. & Arculus, R. J. 1975 *J. Geol.* **83**, 721–736.
- De Paolo, D. J. & Wasserburg, G. J. 1976 *Geophys. Res. Lett.* **3**, 743–746.
- Dosso, L. 1977 Thesis, University of Rennes.
- Duncan, R. A. & Compston, W. 1976 *Geology* **4**, 728–732.
- Dupré, B., Hamelin, B., Allègre, C. J. & Manhès, G. 1978 In *4th Int. Conf. Geochron. Cosmochron. Isotope Geology*, Aspen, Colorado, pp. 103–105.
- Engel, A. E. J. & Engel, C. G. 1964 *Science, N.Y.* **144**, 1330–1333.
- Erlank, A. J., Kable, E. J. D. 1976 *Contr. Miner. Petr.* **54**, 281–291.
- Ewart, A., Brothers, R. N. & Mateen, A. 1977 *J. Volcan. geotherm. Res.* **2**, 205–250.
- Flower, M. F. J., Schmincke, H.-U. & Bowman, H. 1976 *J. Volcan. geotherm. Res.* **1**, 127–147.
- Gast, P. W. 1968 *Geochim. cosmochim. Acta* **32**, 1057–1086.
- Gast, P. W. 1969 *Earth planet. Sci. Lett.* **5**, 353–359.
- Gast, P. W., Tilton, G. R. & Hedge, C. E. 1964 *Science, N.Y.* **145**, 1181–1185.
- Gorton, M. P. 1977 *Geochim. cosmochim. Acta* **41**, 1257–1270.
- Green, D. H. 1971 *Phil. Trans. R. Soc. Lond. A* **268**, 707–725.
- Green, D. H. & Liebermann, R. C. 1976 *Tectonophysics* **32**, 61–92.
- Hamilton, P. J., O'Nions, R. K. & Evensen, N. M. 1977 *Earth planet. Sci. Lett.* **36**, 263–268.
- Hart, S. R. 1976 In *Initial reports of the Deep Sea Drilling Project*, vol. 34, pp. 283–288. Washington: U.S. Government Printing Office.
- Hart, S. S. & Brooks, C. 1977 *Contr. Miner. Petr.* **61**, 109–128.
- Hawkesworth, C. J., Norry, M. J., Roddick, J. C. & Vollmer, R. 1978 In *4th Int. Conf. Geochron. Cosmochron. Isotope Geology*, Aspen, Colorado, pp. 162–164.
- Hawkesworth, C. J., O'Nions, R. K., Pankhurst, R. J., Hamilton, P. J. & Evensen, N. M. 1977 *Earth planet. Sci. Lett.* **36**, 253–262.
- Hofmann, A. W. & Hart, S. R. 1978 *Earth planet. Sci. Lett.* **38**, 44–62.
- Jahn, B.-M. & Nyquist, L. E. 1976 In *The early history of the Earth* (ed. B. F. Windley), pp. 55–76. J. Wiley.
- Jahn, B.-M., Auvray, B., Blais, S., Capdevila, R., Cornichet, J., Vidal, J. F. & Hameurt, J. 1979 *J. Petr.* (In the press.)
- Kanasewich, E. R. 1962 *Geophys. J. R. astr. Soc.* **7**, 158–168.
- Kay, R. 1975 *Trans. Am. geophys. Un.* **56**, 1077.
- Kay, R. W. 1977 In *Island arcs, deep sea trenches, and back-arc basins* (ed. M. Talwani & W. Pitman) (Maurice Ewing Series, 1), pp. 229–242. Washington, D.C.: American Geophysical Union.
- Kay, R. W. 1978 *J. Volcan. geotherm. Res.* **4**, 117–132.
- Kay, R. W. & Gast, P. W. 1973 *J. Geol.* **81**, 653–682.
- Kay, R., Hubbard, N. J. & Gast, P. W. 1970 *J. geophys. Res.* **75**, 1585–1613.
- Kay, R. W. & Hubbard, N. J. 1978 *Earth planet. Sci. Lett.* **38**, 95–116.
- Kay, R. W., Sun, S.-S. & Lee-Hu, C.-N. 1978 *Geochim. cosmochim. Acta* **42**, 263–273.
- Kempe, D. R. C. 1973 *Bull. Br. Mus. (nat. Hist.) Mineral.* **2**, 335–376.
- Kempe, D. R. C. & Schilling, J.-G. 1974 *Contr. Miner. Petr.* **44**, 101–115.
- Klerkx, J., Deutsch, S. & DePaepe, P. 1974 *Contr. Miner. Petr.* **45**, 107–118.
- Lancelot, J. R., Briquieu, L., Westphal, B. & Tatsumoto, M. 1978 In *4th Int. Conf. Geochron. Cosmochron. Isotope Geology*, Aspen, Colorado, pp. 240–241.
- Le Maitre, R. W. 1962 *Bull. geol. Soc. Am.* **73**, 1309–1340.
- Liou, J. G. 1974 *Bull. geol. Soc. Am.* **85**, 1–10.
- Lo, H. H. & Goles, G. G. 1976 *Lithos* **9**, 149–159.
- Lugmair, G. W., Marti, K., Kurtz, J. P. & Scheinin, N. B. 1976 *Proc. Lunar Sci. Conf. 7th*, pp. 2009–2033.
- Mattinson, J. M. 1972 *Analyt. Chem.* **44**, 1715–1716.
- McCulloch, M. T. & Wasserburg, G. J. 1978 *Science, N.Y.* **200**, 1003–1011.
- McDougall, I. 1964 *Bull. geol. Soc. Am.* **75**, 107–128.
- Meijer, A. 1976 *Bull. geol. Soc. Am.* **87**, 1358–1369.
- Meijer, A., Rooke, S., Ruth, J. & Matuska, M. 1978 *Abstr. geol. Soc. Am.* **10**, 137.
- Miyashiro, A., Shido, F. & Ewing, M. 1969 *Contr. Miner. Petr.* **23**, 38–52.
- O'Nions, R. K., Hamilton, P. J. & Evensen, N. M. 1977 *Earth planet. Sci. Lett.* **34**, 13–22.
- O'Nions, R. K. & Pankhurst, R. J. 1973 *Earth planet. Sci. Lett.* **21**, 13–21.

- O'Nions, R. K. & Pankhurst, R. J. 1974 *J. Petr.* **15**, 603–634.
- Oversby, V. M. 1969 Ph.D. thesis, Columbia University.
- Oversby, V. M. 1971 *Earth planet. Sci. Lett.* **11**, 401–406.
- Oversby, V. M. 1972 *Geochim. cosmochim. Acta* **36**, 1167–1179.
- Oversby, V. M. & Ewart, A. 1972 *Contr. Miner. Petr.* **37**, 181–210.
- Oversby, V. M. & Gast, P. W. 1968 *Earth planet. Sci. Lett.* **5**, 199–206.
- Oversby, V. M. & Gast, P. W. 1970 *J. geophys. Res.* **75**, 2097–2114.
- Oversby, V. M., Lancelot, J. & Gast, P. W. 1971 *J. geophys. Res.* **76**, 3402–3413.
- Philpotts, J. A., Martin, W. & Schnetzler, C. C. 1971 *Earth planet. Sci. Lett.* **12**, 89–96.
- Pushkar, P. 1968 *J. geophys. Res.* **73**, 2701–2719.
- Reed, B. & Lanphere, M. 1973 In *Arctic geology* (ed. M. Pitcher) (Am. Ass. Petrol. Geologists Mem. 19), pp. 421–428.
- Rennick, W. L. 1973 M.A. thesis, University of California, Santa Barbara.
- Ringwood, A. E. 1974 *J. geol. Soc. Lond.* **130**, 183–204.
- Schilling, J.-G. 1978 *Trans. Am. geophys. Un.* **59**, 409.
- Schmincke, H.-U. 1975 In *Ecology and biogeography of the Canary Islands* (ed. G. Kunkel), pp. 65–185. The Hague: Junk.
- Scholl, D., Greene, H. G. & Marlow, M. 1970 *Bull. geol. Soc. Am.* **81**, 3583–3592.
- Shih, C. Y., Sun, S.-S., Liou, J. G., Yen, T. P., Rhodes, J. M. & Hsu, I. C. 1972 *Eos* **53**, 535.
- Sinha, A. K. & Hart, S. R. 1972 *Carnegie Instn Wash. Yb.* **71**, 309–312.
- Sun, S.-S. 1973 Ph.D. thesis, Columbia University.
- Sun, S.-S. & Hanson, G. N. 1975a *Geology* **3**, 297–302.
- Sun, S.-S. & Hanson, G. N. 1975b *Contr. Miner. Petr.* **52**, 77–106.
- Sun, S.-S. & Hanson, G. N. 1976 *Geology* **4**, 626–631.
- Sun, S.-S. & Jahn, B.-M. 1975 *Nature, Lond.* **255**, 527–530.
- Sun, S.-S. & Nesbitt, R. W. 1977 *Earth planet. Sci. Lett.* **35**, 429–448.
- Sun, S.-S. & Nesbitt, R. W. 1978 *Contr. Miner. Petr.* **65**, 301–325.
- Sun, S.-S., Nesbitt, R. W. & Sharaskin, A. Y. 1979 *Earth planet. Sci. Lett.* (In the press.)
- Sun, S.-S., Shih, C.-Y. & White, W. M. 1980 (In preparation.)
- Sun, S.-S., Tatsumoto, M. & Schilling, J.-G. 1975 *Science, N.Y.* **190**, 143–147.
- Swainbank, I. G. 1967 Ph.D. thesis, Columbia University.
- Tatsumoto, M. 1966a *Science, N.Y.* **153**, 1094–1101.
- Tatsumoto, M. 1966b *J. geophys. Res.* **71**, 1721–1733.
- Tatsumoto, M. 1969 *Earth planet. Sci. Lett.* **6**, 369–376.
- Tatsumoto, M. 1978 *Earth planet. Sci. Lett.* **38**, 63–87.
- Tatsumoto, M. & Knight, R. J. 1969 *Geochem. J.* **3**, 53–86.
- Tatsumoto, M., Knight, R. J. & Allègre, C. J. 1973 *Science, N.Y.* **180**, 1279–1283.
- Vidal, P. & Dosso, L. 1978 *Geophys. Res. Lett.* **5**, 169–172.
- Vinogradov, A. P., Udintsev, G. B., Dmitriev, L. V., Kanaev, V. F., Neprochnov, Y. P., Petrova, G. N. & Rikunov, I. N. 1969 *Tectonophysics* **8**, 377–401.
- Wasson, J. T. & Chou, C.-L. 1974 *Meteoritics* **9**, 69–84.
- Welke, H., Moorbath, S. & Cumming, G. L. 1968 *Earth planet. Sci. Lett.* **4**, 221–231.
- White, W. M. 1977 Ph.D. thesis, University of Rhode Island.
- White, W. M. & Schilling, J.-G. 1978 *Geochim. cosmochim. Acta* **42**, 1501–1516.
- White, W. M., Schilling, J.-G. & Hart, S. R. 1976 *Nature, Lond.* **263**, 659–663.
- Wood, D. A., Tarney, J., Varet, J., Saunders, A. D., Bougault, H., Joron, J. L., Treuil, M. & Cann, J. R. 1979 *Earth planet. Sci. Lett.* **42**, 77–97.
- Yen, T. P. 1958 *Taiwan Min. Indus.* **11**, 16–23.
- Yen, T. P. 1970 *Proc. geol. Soc. China* no. 13. pp. 51–62.
- Zartman, R. E. & Tera, F. 1973 *Earth planet. Sci. Lett.* **20**, 54–66.
- Zindler, A., Brooks, C., Arndt, N. T. & Hart, S. 1978 In *4th Int. Conf. Geochron. Cosmochron. Isotope Geology*, Aspen, Colorado, pp. 469–471.